



HAL
open science

Long term evolution and internal architecture of a high-energy banner ridge from seismic survey of Banc du Four (Western Brittany, France)

Marcaurelio Franzetti, Pascal P. Le Roy, Thierry Garlan, David Graindorge, Alexey Sukhovich, Christophe Delacourt, Nicolas Le Dantec

► To cite this version:

Marcaurelio Franzetti, Pascal P. Le Roy, Thierry Garlan, David Graindorge, Alexey Sukhovich, et al.. Long term evolution and internal architecture of a high-energy banner ridge from seismic survey of Banc du Four (Western Brittany, France). *Marine Geology*, 2015, 369, pp.196-211. 10.1016/j.margeo.2015.08.019 . insu-01200511

HAL Id: insu-01200511

<https://insu.hal.science/insu-01200511>

Submitted on 16 Sep 2015

HAL is a multi-disciplinary open access archive for the deposit and dissemination of scientific research documents, whether they are published or not. The documents may come from teaching and research institutions in France or abroad, or from public or private research centers.

L'archive ouverte pluridisciplinaire **HAL**, est destinée au dépôt et à la diffusion de documents scientifiques de niveau recherche, publiés ou non, émanant des établissements d'enseignement et de recherche français ou étrangers, des laboratoires publics ou privés.

1 Long term evolution and internal architecture of a high-energy banner ridge from
2 seismic survey of Banc du Four (Western Brittany, France)

3

4 Marcaurelio Franzetti¹, Pascal Le Roy¹, Thierry Garlan², David Graindorge¹, Alexey
5 Sukhovich¹, Christophe Delacourt¹, Nicolas Le Dantec¹

6

7 ¹ Université Européenne de Bretagne Occidentale, UMR-6538 Domaines Océaniques,
8 IUEM / CNRS. Place Copernic, 29280 Plouzané, France. E-mail:
9 marcaurelio.franzetti@hotmail.fr, 00 33 2 98 49 87 17

10 ² SHOM, DO/HOM/REC-CFuD/Sédimentologie, 13, rue du Chatellier 29228 Brest,
11 France

12 Abstract

13 The recent completion of a coupled seismic and swath bathymetric survey, conducted
14 across the sand ridge system of the *Banc du Four* located on the Atlantic continental shelf of
15 Brittany (Mer d'Iroise, France), provided new data for the study of the long term evolution of
16 deep tidal sand ridges. Five seismic units are distinguished within the ridge, separated by
17 pronounced major bounding surfaces. The basal unit is interpreted to be shoreface deposits
18 forming the core of the ridge. It is overlaid by a succession of marine sand dunes fields
19 forming the upper units. Sandwave climbing, which combines progradation and accretion, is
20 the major process controlling the growth of the ridge. The elevation of the preserved dune
21 foresets reaches values of about 20 to 30 m within the ridge. The foresets indicate a
22 combination of giant dunes characterized by numerous steep (up to 20°) clinoforms
23 corresponding to a high-energy depositional environment. Moreover, the presence of scour
24 pits linked to the 3D geometries of giant dunes allow the growth of bedforms migrating
25 oblique to the orientation of giant dune crest lines. All of the radiocarbon ages of the biogenic
26 surficial deposits of the *Banc du Four* range from 10,036 to 2,748 cal years B.P. and suggest

27 the *Banc du Four* has grown during the last sea-level rise. The apparent absence of recent
28 surface deposits could be caused by a change in benthic biogenic productivity or the non-
29 conservation of recent deposits. In contrast, the presence of relatively old sands at the top of
30 the ridge could be explained by the reworking and leakage of the lower units that outcrop
31 locally at the seabed across the ridge. Moreover, the long-term evolution of the ridge appears
32 strongly controlled by the morphology of the igneous basement. The multiphase accretion of
33 the ridge is closely linked to the presence of a residual tidal current eddy, consecutive with
34 the progressive flooding of the coastal promontories and straits that structured the igneous
35 basement.

36 Therefore, the *Banc du Four* should be thought of as a representative example of a
37 large-scale high-energy banner bank.

38 1. Introduction

39 Sand ridges (or sand banks) are the most significant bedforms of tidal-dominated
40 continental shelves. These elongated bedforms are flow-parallel or slightly oblique ($<30^\circ$) to
41 the peak of tidal flow direction (Van Veen, 1936; Kenyon and Stride, 1970; Kenyon et al.,
42 1981; Belderson et al., 1982; Le Bot, 2001). They result from sand-transporting
43 hydrodynamics and typically exhibit kilometric length and decametric height (Trentesaux et
44 al., 1999; Berthot and Pattiaratchi, 2006). In this study the *Banc du Four*, a particular
45 example of sand ridges located at the junction area between the English Channel and the
46 North Atlantic Ocean, is investigated. Numerous types of tidal sand ridges are observed
47 throughout the English Channel and the Celtic Sea. According to the classification system of
48 Dyer and Huntley (1999) (modified by Kenyon and Cooper, 2005), their morphodynamic
49 processes allow us to distinguish (1) open shelf ridges, (2) estuary and delta mouth bars, and
50 (3) banner sand ridges or “banner banks”. Open shelf ridges are the largest and deepest
51 sandbanks, oriented at angle to the flow (Deleu et al., 2004). They have been mostly studied
52 on the outer continental shelf of the Celtic Sea (Bouysse et al., 1975; Reynaud, 1996;
53 Tessier, 1997; Berné et al., 1998; Marsset et al., 1999). Estuary mouth bars lie parallel to the

54 flow, and are associated with macrotidal tide-dominated estuaries, for example Mont Saint
55 Michel and the Seine bays on the southern English Channel (Tessier et al., 2010). Finally,
56 banner sand ridges (Neill and Scourse, 2009) are attributed to the presence of residual
57 current eddies generated by the tidal flow passing a coastal irregularity (Davies et al., 1995)
58 or island (Wolanski et al., 1984). They are well illustrated on the Shambles bank along the
59 Dorset coast in the U.K. (Bastos et al., 2003) and on the Schole and Sercq banks on the
60 coast of France (Quesney, 1983; M'Hammdi, 1994; Walker, 2001).

61 Moreover, if most of the superficial morphologies of ridges appear to be in equilibrium
62 with the present-day hydrodynamic regime, the time-scales of the processes responsible for
63 the formation and evolution of these large bedforms are of the same order as the duration of
64 a high frequency sea-level cycle and most of them are transgressive features (Reynaud et
65 al., 2003; Reynaud and Dalrymple, 2012). Furthermore, physical models have shown the
66 interplay of the substratum with the presence of a small bed perturbation during ridge
67 initiation (Huthnance, 1973, 1982a, 1982b). These models argue for a continuum between
68 juvenile and constructional (fully evolved) ridges as conditions change over a transgression
69 (Snedden and Dalrymple, 1999). This implies that sea-level fluctuation, particularly during the
70 last post-glacial sea-level rise, is one of the main controlling factors of the long-term evolution
71 of tidal ridges, along with nature, source of sediment supply, and paleomorphology. As a
72 consequence of both the long and short-term combined processes involved in tidal ridge
73 development, the understanding of ridge morphodynamics is needed to characterize their
74 internal architecture.

75 Several previous studies have already dealt with internal ridge architecture on
76 continental shelves (Houbolt, 1968; M'Hammdi et al., 1992; Berné et al., 1994, 1998;
77 Tessier, 1997; Marsset et al., 1999; Reynaud et al., 1999a, 1999b, 2003; Trentesaux et al.,
78 1999; Bastos et al., 2003; Olariu et al., 2012; Vecchi et al., 2013), however most of them
79 focused on shallow waters (0-50 m Lower Astronomical Tide, L.A.T.) or concerned
80 themselves with the moribund ridges located on the outer shelf at depths below that of the
81 Last Glacial Maximum sea-level drop (> -120 m). Other studies were concerned with tidal

82 ridges at intermediate depths but in specific highly-supplied sedimentary environments such
83 as the Yellow Sea and East China Sea (Jung et al., 1998; Berné et al., 2002; Jin and
84 Chough, 2002).

85 The lack of studies on the long-term evolution of the sand ridge system of the *Banc du*
86 *Four*, located on the starved continental shelf of western Brittany, motivated the coupled
87 seismic and swath bathymetric surveys. This tidal sand ridge system is about 45 m thick,
88 settled by depths of 70 to 105 m L.A.T., and surrounded by straits and islands. Results of a
89 study on its short-term evolution have already been published and have shown that this ridge
90 does not display classic ridge morphology (Franzetti et al., 2013). The aim of this paper is thus
91 to present the results of these surveys. We discuss the relative influences of intrinsic
92 sedimentary parameters and hydro-sedimentary processes, as well as post-glacial
93 transgression and shelf paleomorphology in regards to tidal sand ridge growth.

94 2. Ages and stratigraphic modelling of tidal ridge growth

95 There is very little data concerning the dating of tidal ridges, due to the difficulties of
96 coring sand bodies and the fact that the penetration of vibrocorers is usually limited to about
97 5 m. As a consequence, the timing of tidal ridge genesis remains speculative in most case
98 studies.

99 Generally, the growth of ridges is believed to be linked to the post-glacial sea-level rise
100 and thus considered to be younger than 20 ka. This assumption is in accordance with the
101 ages (9,000 to 1,300 years B.P.) of the detritic gravels and bioclastic sands recovered at the
102 base and top of the tidal ridges of the Western English Channel (Hommeril, 1971; Auffret et
103 al., 1980; M'Hammdi, 1994). Tidal ridges of the southern North Sea also originated at around
104 8,000 to 7,800 years B.P. (Jelgersma, 1979; Trentesaux et al., 1999). They can be
105 considered as linked to the post-glacial sea-level rise and the start of their formation depends
106 on the age of their basement flooding. The deeper ridges are formed early, and seem to
107 record strong ravinement by tidal currents that remove the main part of the early deposits. As
108 the sea level rises, the tidal control becomes weaker and the ridge surface becomes wave

109 dominated above a wave ravinement surface (Huthnance, 1982b; Reynaud et al., 2003). In
110 contrast, the shallower tidal ridges are formed later and may preserve initial lower coastal
111 deposits and tidal-dominated deposits that are located at the upper parts of the ridge (Berné
112 et al., 1994). Alternatively, deeper tidal ridges could also be considered as mainly consisting
113 of lowstand deposits (*i.e.* older than 20 ka) and only their top could correspond to
114 transgressive deposits fed by erosional process. This interpretation is given by Berné et al.
115 (1998) for the tidal ridges of the Celtic Sea. The ridge itself is assumed to be a partially relict
116 feature created during periods of sea-level lowstand; its surface is still active, exhibiting
117 attached dune fields in accordance with present hydrodynamics. The report on sands dated
118 from MIS2 and recovered by vibrocoreing across the Celtic Banks (Evans, 1990) reinforces
119 this hypothesis.

120 3. Study area and previous results

121 The study area (Fig. 1A) is located about 10 km off the shore of western Brittany
122 (France) and extends into the northern part of the Iroise Sea (48°30'N, 05°00'W). The water
123 depth ranges from 70 to 105 m L.A.T. The area is characterized by strong tidal currents and
124 large swells. Indeed, the singular morpho-bathymetry of this segment of Brittany's continental
125 shelf consists of a wide, northward-opened triangular bay that catalyses and amplifies tidal
126 dynamics (Franzetti et al., 2013). It is bound to the east by coastal reefs (plutonic rocks) and
127 to the south and west by the Ushant-Molene Archipelago. This barrier is interrupted by two
128 narrow, shallow straits, the Fromveur strait (60 m L.A.T.) and the Four strait (13 m L.A.T.),
129 whereby tidal current eddies become strong alternating unidirectional currents with surface
130 velocities reaching up to 4 m.s⁻¹ (Hirschberger, 1962a, 1970). Moreover, Eulerian residual
131 tidal currents, modelled by Guillou (2007) and the French Operational Coastal
132 Oceanographic Centre PREVIMER, reveal a clockwise current eddy occurring in the western
133 part of the study area where a dominant north-eastward current extends along the coastal
134 Four strait to the east (Fig. 1B). The area is also exposed to Atlantic storm waves coming
135 from the northwest. Their heights regularly exceed 4 m, with wavelengths reaching over 200

136 m (Dehouck, 2006). The frequent rough seas could explain the limited number of studies
137 devoted to the *Banc du Four*. The first survey was conducted by Hirschberger (1962b) and
138 enabled the definition of the approximate morphology of the area and highlighted the
139 massive volume of sand deposits. It also revealed the carbonate nature of the sediments,
140 which are predominantly composed of organogenic debris with a mean grain size of about
141 0.8 to 0.9 mm. A recent study based on the completion of three recent 29-month-spaced
142 swath bathymetric surveys of the area, complemented by a historical data set, enabled the
143 accurate characterization of morphology and the quantification of dune migration rates
144 (Franzetti et al., 2013; Franzetti, 2014):

145 Concerning the morphology and equilibrium conditions, the recent surveys have shown
146 that the *Banc du Four* bedform field is characterized by offshore sandbodies that define a V
147 shape. More than 500 large dunes exhibit a great diversity of morphologies, ranging from 2D
148 to 3D shapes. The largest dune (over 1000 m in wavelength and over 30 m in height)
149 reaches the maximum size of the sedimentary structures recently described in the Irish Sea
150 (Van Landeghem et al., 2012), where the tidal regime and depths are quite similar to those of
151 Brittany's continental shelf (Figs. 2A, 2B). Previous results have shown that the outer limits of
152 the *Banc du Four* have remained unchanged during the last 82 years. Despite the fact that
153 the imprecision of the ancient data set prevents the assessment of vertical movement, the
154 comparison of the respective locations of the 50 m isobath shows that the southern flank of
155 the sand ridge has eroded, whereas the eastern part has accreted (Franzetti et al., 2013).

156 Concerning dune migration, the rates calculated for the eastern part of the *Banc du*
157 *Four* range from 3 m.a⁻¹ to 20 m.a⁻¹. Such velocities have never before been previously
158 recorded on deep continental shelves (>70 m) and attest to the existing morphodynamic
159 equilibrium of the large dunes (Franzetti et al., 2013). Actually, the non-consistent
160 morphology and orientation of the sand ridge could be partially explained if it is considered
161 as being inherited and shaped by different hydrodynamic settings during the last post-glacial
162 stage.

163 4. Data and methods

164 The *Banc du Four* sand ridge was investigated by a series of High and Very High
165 Resolution seismic surveys (GeoBrest 2003, 2005, 2006, 2010, 2012, and 2013) carried out
166 by the “Institut Universitaire Européen de la Mer” (IUEM, UBO) from onboard the
167 oceanographic research vessel (R/V) “Côtes de la Manche”. The seismic energy sources
168 were a 250J SIG™ mille® supplying a SIG™ EDL1020® spark-array with 200 strands, and a
169 50J SIG™ENERGOS supplying a 50 strand spark-array. Seismic receivers were composed
170 of a monochannel streamer for GeoBrest 2012 and a 6-channel streamer, SIG™ 16 for the
171 other surveys. The seismic grid consisted of 47 seismic profiles with a variable spacing of
172 100 to 1000 m (Fig. 3). IXSEA™ Delph2.1® software was used to acquire and process the
173 data. Interpretation was performed using SMT™ KINGDOM®. Time-depth conversions are
174 estimated in the text using a seismic velocity of 1600 m.s⁻¹ in porous sands.

175 The superficial sedimentology of the sand ridge was studied by the analysis of 50
176 Shipek grab samples taken during the GeoBrest 2010 survey. Samples were washed and
177 dried before analysis. Sedimentological parameters (mean grain size, sorting, and skewness)
178 according to Folk and Ward (1957) have been calculated by weighing different fractions split
179 by vibro-sieving. Carbonate content was measured with a Bernard calcimeter using the
180 volumetric calcimetric method. The radiocarbon method was used to date seven shells
181 originating from five samples. AMS ¹⁴C dating was performed on shells by the Poznan
182 Laboratory (Tab. 1; Fig. 4).

183 Absolute dates have been calibrated using the programme Calib Rev7.1. We used the
184 marine radiocarbon calibration curve “Marine09” for marine shell samples (Reimer et al.,
185 2009). These calibrations yield ages with 1 standard deviation (1 sigma, 68.3% confidence
186 level; 2 sigma, 95.4% confidence level). We applied a regional deviation ΔR of -40 ± 42 years
187 corresponding to the nearby Sein Island (Marine reservoir correction database:
188 <http://intcal.qub.ac.uk/marine/>).

189 5. Results and Interpretation

190

5.1. Samples

191 The surface of the *Banc du Four* is composed of slightly gravelly (Folk and Ward, 1957)
192 bioclastic sands (Fig. 2B). The mean grain size (M) varies between 0.27 and 4.3 mm with an
193 average value of 0.89 mm. The calcimetry analyses show that the sand consists of 80%
194 carbonates, with values ranging from 16 to 95%. The carbonate fraction is composed of shell
195 ash and the shells of bivalves (20%, belonging to the families Arcidae, Glycymeridae, and
196 Veneridae, urchin spicules (27%), gastropods (3%), bryozoan (5%, mostly Cellaria), Polychet
197 (2%), crab carapaces debris (2%), and algae (1%). Undetermined bioclastic debris makes
198 up 40%. The terrigenous fraction (20%) is composed of gravels, including granite clasts,
199 quartz, and flint. There are two sediment types on the sand ridge: Type 1 corresponds to the
200 majority of samples, and is characterized by medium to coarse (M between 0.25 and 1 mm)
201 sand, moderately sorted (σ_1 between 0.5 and 1). The carbonate fraction is largely dominant
202 (higher than 85%). Type 2 is in the minority and corresponds to samples 8 and 9 located in
203 the east. Type 2 samples are characterized by siliciclastic gravel (M between 2 and 4 mm),
204 including granitic large pebbles. This sediment is poorly sorted (σ_1 between 1.5 and 2). The
205 carbonate fraction is lower than 25%, characterized by large, well-preserved bivalve shells.

206

5.2. Seismic

207 The architecture of the *Banc du Four* was principally examined using VHR sparker
208 surveys.

209 Three seismic units (U_{S1} to U_{S3}) are identified within the substratum of the sand
210 bedforms, and five (U_{B1} to U_{B5}) are identified within the ridge. They are separated by
211 pronounced, regional-scale erosional unconformities distinguished on the seismic lines at the
212 scale of the ridge. They are shown by selected representative sections (Fig. 3). These unit
213 boundaries can be considered to be major bounding boundaries or first-order discontinuities
214 within the ridge by comparison to previous works on eolian dunes (Brookfield, 1977), tidal
215 sand dunes (Berné et al., 1988, 1989, 1993; Le Bot and Trentesaux, 2004; Ferret et al.,
216 2010), and sand ridges (Marsset et al., 1999; Trentesaux et al., 1999). The corresponding

217 reflectors are labelled on the seismic lines (R_{B1} to R_{B4}) and mark the respective upper limits
218 of the seismic units U_{B1} to U_{B4} .

219 Each unit shows local geometric and facies variations and can be described as an
220 assemblage of subunits, each composed of migrating or aggrading bedforms with internal
221 medium bounding surfaces that can only be locally followed (second order discontinuities)
222 within the ridge. The seismic reflectors within the sub-units are assumed to be the
223 isochronous surfaces of short-term sediment transport. They roughly correspond to
224 reactivation surfaces, i.e., discontinuities in the lateral sequence of cross-strata within the
225 unit, with either a planar or convex up erosion surface. They are representative of the
226 lithology and energy variations. The spatial distributions of the sand ridge seismic units are
227 shown on the isopach maps (Fig. 5). Correlation of the seismic units described below and the
228 sediment samples are shown in Fig. 4.

229 5.2.1. Basement

230 The basal unit U_{S1} is characterized by a chaotic seismic facies interpreted as being
231 representative of the Hercynian crystalline rocks that outcrop along the nearby Ushant-
232 Molene Archipelago (Fig. 3). This crystalline basement is structured by regional-scale faults
233 marked on the bathymetry by a succession of straits (Fromveur and Four, see §3), where
234 morphologic thresholds communicate with deeper domains along the Ushant-Molene
235 Archipelago. Above, the spatial arrangement of the reflectors of the U_{S2} unit defines complex
236 oblique-parallel-to-sigmoidal patterns with numerous imbricated erosional surfaces. The U_{S2}
237 unit merges at the seabed towards the northeast and chronostratigraphic identification of the
238 deposits is possible from previous studies conducted along the continental shelf (Andrieiff et
239 al., 1972; Lapierre and Bouysse, 1975). They are considered to be biogenic Miocene
240 deposits and could correspond with the calcarenites from the Cockburn Formation identified
241 along the Western Approaches (Evans, 1990; Le Roy et al., 2011). The upper unit U_{S3}
242 exhibits reflectors ranging from chaotic to oblique clinoforms, suggesting a channel-fill
243 geometry (Fig. 6). The corresponding deposits define the infill of a deep paleo-valley 200 to

244 400 m wide and 30 m deep, located along the previous bounding fault, its geometry seems to
245 be controlled by the topography of the bedrock (U_{S1}). The valley was probably the outer
246 segment of a fluvial network that has drained the coastal rias of NW Brittany and was
247 extended further offshore up to the 200 m deep Ushant Trough. As in the other case studies
248 done along the French Atlantic margin (Chaumillon et al., 2011), the valley fill is assumed to
249 correspond to the Pleistocene sequence (Fig. 7).

250 5.2.2. Sand ridge

251 Unit U_{B1}

252 *Description.* The basal unit (U_{B1}) is located at the sole of the present-day sand ridge. It
253 settled over the Neogene deposits and the igneous basement topped by the R_{B0} reflector. Its
254 lower boundary lies at about 110 and 120 ms TWT (i.e. about 85 to 95 m b.s.l.). It consists of
255 several small patchy deposits, lenticularly-shaped, and connected with each other forming a
256 basal sole lying over the basement units. Its thickness is generally lower than 10 ms (about 8
257 m) and it extends to the north of the crystalline rock aprons (U_{B1}), showing an elevation of
258 about 20 m above the surrounding seabed (Fig. 5, U_{B1}). Where the unit is thick enough, the
259 internal reflectors show an oblique parallel pattern dipping up to 5° northward (NNE to NNW),
260 (Fig. 8).

261 *Interpretation.* The northwest dip of the bedding planes, the low elevation of the unit
262 above the basement, and its elongation toward the NNE all suggest that these deposits
263 nucleated behind the rock aprons. These types of sediment arrangements showing through
264 cross beddings are well-matched with shoreface deposits and we interpret the corresponding
265 deposits as being representative of high energy coastal deposits.

266 Unit U_{B2}

267 *Description.* This unit constitutes the bulk of the south-eastern side of the sand ridge.
268 The correlation of seabed samples with the seismic units that outcrop at the seabed show
269 that the U_{B2} unit mainly corresponds to siliciclastic gravels. It extends north-eastward and
270 delineates an elongated prism parallel to the eastern dune field of the *Banc du Four*. Its

271 southern termination is anchored along the rocky apron. Its maximum thickness is 45 ms
272 TWT (about 35 m), and its top is at about 60 m (below sea level, b.s.l.) Its eastern and
273 southern flanks outcrop directly at the seabed, while its northern and western ridges are
274 buried by units U_{B3} to U_{B5} . The geometries of the medium-to-high amplitude reflectors are
275 imbricated sets showing clinoform profiles (Fig. 3). Two sets are clearly individualized along
276 the SW-NE and exhibit high angle reflectors (from 5° to 15° to the northeast).

277 *Interpretation.* The current direction is indicated by the northward elongated shape of
278 the unit and the presence of stacked sets of high angle cross-stratification assumed to be
279 formed by dunes that migrate in this direction. The sets delineate stacked, lens-shaped
280 bodies bounded by gently undulating concave bounding surfaces. The top sets are absent
281 along the erosional upper unit-bounding surface (R_{B2}) that outcrops at the seabed to the
282 south. Along the WWN-EES transverse seismic profiles, the medium bounding surfaces are
283 slightly concave upwards (Fig. 9). The U_{B2} unit is thus interpreted to be downstream-
284 accreting large-scale compound dunes (Dalrymple and Rhodes, 1995). The transverse WWN
285 dipping concave surfaces produced scallop-shaped sets of cross-beds (Rubin and Hunter,
286 1982). They are assumed to represent the progressive infilling of space between dunes that
287 approach each other and for which both sides of the hollow are the stoss and lee sides of the
288 two facing bedforms. The elevation of the preserved dune foresets is about 15 to 20 m. If we
289 consider the present day Brittany shelf to be where the highest dunes (30 m) tend to scale to
290 flow depth at a ratio of about 1:3 (Franzetti et al., 2013; Franzetti, 2014), it is probable that
291 the water would have been about 45 to 60 m deep during the deposition of U_{B2} . These
292 deducted values are much less than what is predicted by the equation of Yalin (1964) which
293 stated a ratio of 6:1 between water depth and dune height.

294 Unit U_{B3}

295 *Description.* It forms a large part of the western section of the sand ridge (Fig. 10). It
296 outcrops at the seabed over a small surface at the south of the ridge (Fig. 4). The correlation
297 of sediment samples with seismic units show that U_{B3} , like the upper units, corresponds to

298 bioclastic sands. The U_{B3} unit lies over the basement, or over units U_{B1} and U_{B2} toward the
299 southwest. Its WNW-EES orientation contrasts with the U_{B2} unit, even if its eastern
300 termination trends to parallel to the NNE-SSW orientation of the U_{B2} unit. Its maximum
301 thickness is comparable to the previous unit and its upper boundary is a sharp erosional
302 surface. The unit is made up of numerous superposed sets with thicknesses ranging from 10
303 to 40 ms, bounded by well-marked medium bounding surfaces (Fig. 10). Here, again,
304 geometries consist of oblique-parallel to oblique-tangential profiles with moderate angle
305 dipping reflectors (5 to 10°). The direction of the progradation enables the distinction of two
306 zones within the sand ridge: (1) in the western section the orientation is mostly south-
307 westward; (2) in the eastern section it is north-westward. The basal progradation surfaces
308 separating the overlying clinoforms themselves dip to the north with variable angles (0 to 3°).

309 *Interpretation.* We interpret the geometry of U_{B3} as corresponding to large
310 superimposed dunes. The dipping reflectors in each set are conformable to the lee side of
311 the large dunes and indicate the net migration of large subtidal dunes. The basal
312 progradation surfaces separating cross-beddings delineate climbing dunes with no stoss side
313 preservation, and various angles of climb. They correspond to structures deposited by two-
314 dimensional bedforms climbing at a stoss-erosional, lee-depositional, net-positive angle of
315 climb as defined by Rubin and Carter (2006), and corresponding to A-type or subcritical from
316 Jopling and Walker (1968) and Allen (1970).

317 Another remarkable pattern is observed within the U_{B3} unit. It consists of a large
318 concave-up surface marking the base of a 100 m wide and 25 ms (about 20 m) deep
319 elongated trough observed along the SW-NE seismic sections. Its lateral extension is limited
320 and does not exceed several hundred meters, as deduced from parallel sections. It is filled
321 by south-eastward prograding reflectors with tangential basal contacts that define a
322 perpendicular orientation with respect to the troughs. Its interpretation is discussed later in
323 the text (§2.1).

324 Unit U_{B4}

325 *Description.* The U_{B4} seismic unit forms a 20 m thick prism which has accreted up to
326 the U_{B2} and U_{B3} units (Fig. 3 and Fig. 11). It is characterized by large (several hundred
327 meters of extension), low angle clinoforms (3 to 4°) dipping to the northwest and slightly to
328 the NNE at the southern termination of the unit. The high continuity moderate-to-low
329 amplitude and frequency reflectors downlap over the basal boundary and are truncated at
330 the top. Some local variations of geometry are observed at the western termination of the
331 ridge (line 13-05, Fig. 3) but the pattern of the entire unit is quite consistent over the sand
332 ridge.

333 *Interpretation.* The reflectors of the U_{B4} unit are thus considered to be formed by lateral
334 accretion of the ridge surface. They migrate laterally toward the northwest relative to the
335 ridge axis (NE-SW)

336 Unit U_{B5}

337 *Description.* The uppermost seismic unit, U_{B5} , nearly covers the entire ridge, and
338 corresponds to its present shape (Fig. 12). Its thickness reaches up to about 50 ms TWT
339 (about 40 m) along the northeast area, and is absent in the southeast. The lower bounding
340 surface of the unit is an erosional unconformity that marks a change in the architecture of the
341 deposits. Medium bounding surfaces are frequent within the unit and their characteristics
342 allow us to distinguish two different zones characterized by their geometries. To the west of
343 the ridge, unit U_{B5} corresponds to a succession of aggrading and prograding deposits dipping
344 to an overall southwest direction at angles ranging between 0° to 15°. The thickest sets
345 reach about 30 m. Examination of the western part of the ridge also reveals the presence of
346 deep troughs showing similar sizes to those of unit U_{B3} , and showing an WNW-EES
347 orientation. Their infill consists of large (20-30 m) and high-angle (15 to 20°) clinoforms
348 prograding to the EES and climbing along the western flank of the ridge over the U_{B3} and U_{B4}
349 units. At the eastern section of the ridge, the U_{B5} unit forms a blanket that extends to the
350 NNE. The seismic pattern consists of slightly (1 to 3°) dipping reflectors with the lateral extent
351 reaching 250 m and oriented toward the NNE at the top of the ridge. The NNE extension

352 corresponds to the eastern dune field of the *Banc du Four*. The field is characterized by
353 numerous reactivation surfaces and the directions of the dipping reflectors reflect the present
354 day migration of dunes at the seabed.

355 *Interpretation.* Except for the nature of the troughs discussed below, the pattern of the
356 western part of unit U_{B5} is a continuation of that of the U_{B3} deposits. The U_{B5} deposits are
357 interpreted as a succession of stacked dunes migrating to the southwest and climbing along
358 downlap basal surfaces. These basal surfaces dip 1 - 5° to the NNE. The thickness of the
359 preserved dune foresets is about 20 to 30 m, similar to the giant dunes located southwest of
360 the ridge. The underlying units progressively disappear westward, where a succession of
361 giant asymmetric dunes marks the edge of the ridge. The stratigraphic pattern of these
362 climbing giant dunes shows that the southern deposits are older than the northern dunes.
363 Here again, as for unit U_{B3}, the morphology of the progradation basal surface controls the
364 angle of the lee-side and the bottom set pattern of the superimposed dunes. The angles are
365 more pronounced and the internal reflectors show an oblique parallel pattern where the basal
366 surfaces are flat and horizontal. In contrast, they become sub-horizontal with tangential
367 terminations where the angles of the basal surfaces are higher. On the eastern part of the
368 ridge, the geometry of unit U_{B5} suggests an intense reworking of the ridge crest and a
369 residual north-eastward sediment transport toward the attached dune fields. The transport is
370 in accordance with present hydrodynamics and attests to the active state of the *Banc du*
371 *Four*.

372 Another remarkable feature is the presence of deep troughs within units U_{B3} and U_{B5}
373 (Fig. 12 and Fig. 13). These structures are only located along the western flank of the ridge.
374 Examination of parallel seismic lines indicate that these troughs are quite short (500 m in
375 length), about 200 to 300 m wide, oriented roughly W-E, and pinching out toward the western
376 flank of the ridge. Their shapes are ovoid. The lowest position of the depression is about 90
377 m b.s.l. and corresponds to the basement where the entirety of the sandy bedforms has been
378 removed by erosion. They are interpreted as pits with local scouring separating a giant three-
379 dimensional dune (Rubin, 1987; Reynaud et al., 1999b). Their infill consists of oblique

380 reflectors (angle of dip about 10°, up to 15°) prograding to the EES. They are perpendicular
381 to the pit's flanks and considered to be the bedding of giant tidal dunes. Three to four sets
382 separated by medium bounding can be distinguished within the pit's infills. Crossbedding
383 directions are similar within each set, and downlap over the bounding surfaces. These
384 boundaries correspond to migration surfaces, and the dune foresets show offshoots passing
385 the troughs and reaching the flank of the adjoining dune. This type of bedding feature is quite
386 similar to minor scale, asymmetric, wave ripple cross bedding (Boersma, 1970).

387 This interpretation of the pit's infills leads us to consider the occurrence of a
388 subordinate eastward paleo-current, normal to the polarity of the giant dunes. This is
389 consistent with recent current measurements taken at the seabed along the nearby eastern
390 dune field, from 10/11/2011 to 20/11/2011 during the PROTEVS DUNES Cruise operated by
391 the S.H.O.M. Results show the occurrence of a minor eastward current component able to
392 mobilize middle sands and reaching up to 0.5 m.s⁻¹ at medium tidal range. Therefore it
393 makes sense to consider that sediment transfer is still today partially controlled by a
394 subordinate E-W tidal current along the scour pits area and to look for sedimentary structures
395 related to this direction of sediment transport. Examination of multibeam bathymetric images
396 provided from the 2010 Daurade cruise (Fig. 14) reveal that such structures are located at
397 the junction of the western giant dunes and the sand ridge. Four to five unfilled pits with sizes
398 similar to the structures observed on seismic lines are identified along the troughs separating
399 the giant dunes. They correspond to erosive structures where the basement outcrops at the
400 seabed in the center of the troughs. They are separated one from another by sinuous and
401 oblique dune crests and oriented in a NNW-SSE direction. They are partially connected to
402 the main giant dunes showing sinuous and bifurcated crests. The polarities of the bedforms
403 enable identification of the current pattern, which shows a succession of antagonist gyres
404 and a migration of dunes toward the EES (Fig. 14).

405 The divergence of the oblique bedforms relative to the mean current normal to the
406 orientation of giant dune crest lines is thus controlled by the presence of residual eddies.
407 This situation was demonstrated by flume experiments where bidirectional flows were

408 applied to subaqueous dunes with a divergence angle greater than 90° (Rubin and Ikeda,
409 1990). It is thus consistent with the consideration of an eastward subordinate residual current
410 mentioned above.

411 6. Discussion

412 6.1. Architecture of the sand ridge

413 One of the most remarkable morphological features of the *Banc du Four* is the
414 presence of two large sand dune fields oblique to one another and intersecting around the
415 sand ridge depicted by seismic investigation. This pattern is quite different from the typical
416 shapes of sand ridges proposed by Dyer and Huntley (1999). It reflects the convergence of
417 two tidal bedload transport pathways. One is parallel to the coast and orientated NW-SE, the
418 second corresponds to a gyre generated by the Ushant promontory. Though this tidal-
419 transport path is complex, the *Banc du Four* is clearly anchored by coastal eddies and the
420 sandwaves display a convergent pattern toward its western flank, favouring accretion.

421 Its smooth and rounded crest is perceptible to the east, and its roughly W-E extension
422 is neither parallel nor perpendicular to the residual current, which is oriented towards the
423 northeast (Fig. 2). This morphology means that it cannot be considered representative of an
424 open shelf ridge, normally marked by straight to slightly sinuous crests with orientations at a
425 small oblique angle (about 7 to 15°) to the peak tidal flow direction. However, banner sand
426 ridges are commonly attributed to the presence of a tidal residual current eddy, such as
427 observed here. The *Banc du Four* could be thus considered representative of this type of
428 ridge, even if numerous banner ridges exhibit associated parallel sand ridges (Dyer and
429 Huntley, 1999).

430 Internal structure

431 The vertical succession of the internal structure of the *Banc du Four* is interpreted to be
432 lower coastal deposits grading to offshore deposits and records a sea-level rise. The
433 combination of sandwave climbing processes combining progradation and accretion is the

434 major parameter controlling the growth process of the ridge, as previously described by
435 Reynaud et al., (1999b), Bastos et al. (2003) and Reynaud and Dalrymple (2012). The
436 elevation of the preserved dune foresets is about 20 to 30 m within the ridge and indicates a
437 combination of giant dunes fields as early deposits of the U_{B2} unit. They are characterized by
438 numerous steep (up to 20°) clinofolds that attest to the high-energy depositional
439 environment of this banner bank. Moreover, the presence of scour pits created by the 3D
440 geometries of the giant dunes allow the growth of bedforms migrating oblique to the
441 orientation of the giant dune crest lines.

442 This compound architecture of the *Banc du Four* is different from the first seismic
443 records of the Well Bank and Smith's Knoll (southern North Sea), presented by Houbolt
444 (1968) and for a long time considered representative of the internal structures of sand ridges.
445 This initial model is characterized by slightly inclined reflectors (2 to 4°) related to the
446 migration of the ridge and lying above a flat basal surface. These ridges migrated laterally
447 relative to their axis, due to the obliqueness of the dominant tidal residual flow. Houbolt's
448 theory is effectively validated by more recently studies in the North Sea in relatively shallow
449 waters (< 50 m b.s.l.), and on tidal and storm dominated shelves (Cameron et al., 1992;
450 Davis and Balson, 1992; Meene, 1994). It is also representative of the shoals located around
451 coastal headlands in southern England, where sand streams formed by large sandwaves do
452 not show a convergent pattern toward their crests (Bastos et al., 2003).

453 Nevertheless, the internal structure of the *Banc du Four*, with a sedimentary core
454 forming the lower units and overlain by sandwaves, is also reported in previous studies
455 (D'Olier, 1981; Laban and Schüttenhelm, 1981; Yang and Sun, 1988; Berné et al., 1994;
456 Marsset et al., 1999; Trentesaux et al., 1999; Bastos et al., 2003). The lower units are
457 characterized in these studies by variable seismic facies: deep-angle prograding reflectors
458 (Bastos et al., 2003), low-angle clinofolds (Reynaud et al., 1999b), or sub-horizontal
459 aggrading deposits (Berné et al., 1994; Trentesaux et al., 1999). They are interpreted as
460 markers of sea-level lowstands. In some cases the basal units also developed above
461 erosional structures such as inlets or paleo-valley fills (Berné et al., 1998; Reynaud et al.,

462 1999b; Snedden and Dalrymple, 1999; Trentesaux et al., 1999). As observed for the deep
463 Celtic ridges (Reynaud et al., 1999b) or the shallow Flemish ridges (Trentesaux et al., 1999),
464 the presence of a paleo-valley located at the base of the structure could correspond to the
465 initial source of material removed by erosion, which triggered the initiation of the ridge
466 growth. Moreover, a basal pebble lag (coastal storm deposits), comparable to coarse
467 deposits constituting U_{B1} in this study, is also indicated for the Sercq banner ridge located in
468 the southern English Channel (M'Hammdi, 1994) at a depth of about 50 m. However, the
469 lagoonal or estuarine deposits recovered and found in several ridges located on sheltered or
470 shallow shelves (Trentesaux et al., 1999; Berné, 1999, 2002) are absent in the *Banc du*
471 *Four*. It is more representative of an evolved stage of sand ridges where lower coastal
472 deposits are partially preserved (see §2).

473 Moreover, very few previous studies dealing with the internal architecture of ridges
474 have mentioned the presence of steep and large clinoforms as observed for the *Banc du*
475 *Four*. The studies of the ridges of the North Sea (Middelkerke ridge, Berné et al., 1993;
476 Trentesaux et al., 1999) and the Southern Celtic Sea (Reynaud, 1996; Berné et al., 1998;
477 Marsset et al., 1999) mentioned reflector foresets with a maximum dip of 10°. No higher
478 values are reported for the banner ridge of the Shambles bank along the Dorset coast where
479 the amplitude of tides does not exceed 2 m (much lower than the 7 m for the Four Bank
480 during spring tides) (Bastos et al., 2003). The only other example reporting similar dip angle
481 clinoforms is the Sercq ridge located along the French Cotentin Peninsula towards the south
482 of the English Channel (M'Hammdi, 1994). The hydrodynamical setting of this banner ridge is
483 quite similar to that of the *Banc du Four* (macro-tidal regime and exposed to storm waves).
484 Nevertheless, the total thickness of this ridge is about 25 m with a shallower basement depth
485 (50 m) and the elevation of preserved clinoforms does not exceed 10 m. As a consequence
486 the *Banc du Four* appears to be, despite its significant depth, a representative example of a
487 large-scale high-energy banner bank where large and steep clinoforms are depicted in a
488 modern environment. Similar sand-prone clinoforms have also been described in the
489 stratigraphic record. Generally found in association with fluvial and deltaic systems, they

490 have often been the subject of divergent interpretations (SEPM Clinoform Conference,
491 2008). The *Banc du Four* shows that the internal structure of a banner ridge must also be
492 considered representative of such bedding structures.

493 6.2. Age model

494 Another significant result of this study concerns the radiocarbon ages of the surficial
495 deposits of the *Banc du Four*. Most of the dating was performed on well-preserved to very
496 well-preserved shells, with the exception of samples 10-8V and 10-42, which suggests
497 limited transport and alteration. The calibrated ages range from 10,036 (10-8V) to 2,748 (12-
498 3J) cal years B.P. (Fig. 4). Though normally the oldest age logically corresponds to the most
499 altered sample, some bivalves, such as sample 10-42J, are quite old (7,401-7,288 cal years
500 B.P.), despite their juvenile appearance. All of the measurements that suggest the *Banc du*
501 *Four* dates from the Holocene were obtained from the seven analysed shells.

502 The correlation of seabed samples to the seismic units that outcrop at the seabed show
503 that the U_{B2} unit, located along the eastern flank of the ridge, corresponds to the oldest
504 deposits. The samples consist of siliciclastic gravel with a low biogenic content, as described
505 above. Their age is then contemporaneous with, or older than the shells included (10,036-
506 9,789 cal years B.P.). Ages of the upper units (U_{B3} to U_{B5}) are less indicative of the sampled
507 units; they range from 7,288 to 2,861 cal years B.P. The siliciclastic facies fit with the peri-
508 Armorican pebbly strip (“cailloutis”) and the quartzitic sands previously described off Devon
509 and Cornwall (Bouysse et al., 1979; Evans, 1990). They are considered to be produced by
510 coastal erosion, and most have been brought into the areas by periglacial processes. The
511 examination of heavy minerals contained in these siliciclastic gravels and sands do not
512 reveal gradients or significant transport toward the axis of the Western Channel Basin
513 (Bouysse et al., 1979). In the present study, the granitic pebbles collected in the Shipneck
514 grab can be correlated with the *Granite à deux micas and Toumaline* and the *granite*
515 *migmatique porphyroïde de Landunvez* that outcrop at a distance of 10 to 20 km from the
516 ridge along the NW Brittany coast. The sedimentary source of the U_{B2} unit is thus considered

517 to be local, with minor transport. A similar interpretation could be done for the U_{B1} unit, also
518 shown to be composed of coarse siliciclastic deposits, with regards to its coastal deposit
519 architecture. The biogenic fraction forming the main part of the *Banc du Four* area shows a
520 biological assemblage commonly reported on the Channel continental shelf for the last
521 transgressive cycle (Bouysse et al., 1979; Wilson, 1982; Reynaud et al., 1999b). More
522 specifically, it is representative of fresh coastal thanatocaenoses (Raffin, 2003), however its
523 spatial distribution is widespread across the shallow depths of the Western Channel
524 (Larsonneur et al., 1982). We find that Bryozoans do not form the main component of the
525 bioclastic debris of the ridge, as was reported for the bulk of the sediments off the Brittany
526 coast (Bouysse et al., 1979). The winnowing effects of tidal and wave induced currents that
527 increase on the relatively shallow waters over the ridge and giant dunes could explain this
528 difference. One also notices that convergent tidal transport pathways and peak bed-stress
529 vectors deduced from paleo-tidal modelling increase around 9,000 years B.P. across NW
530 Brittany (Uehara et al., 2006; Reynaud and Dalrymple, 2012) and favour ridge formation in
531 agreement with our observations.

532 Moreover, the westward residual ebb-dominant regional tidal currents (Bouysse et al.,
533 1979; Auffret, 1983; Evans, 1990) are able to transport the bioclastic sands through the NW
534 Brittany continental shelf, and contribute to supply the *Banc du Four*. Nevertheless, this
535 sediment supply is probably not significant, rather the good preservation of juvenile shells
536 suggests a local autochthon origin of the bioclastic sands linked to the tidal gyres that occur
537 around the ridge. It is also difficult to explain the broad spectrum of ages and absence of
538 recent or present surficial deposits. The presence of relatively old sands at the top of the
539 ridge could be explained by the alteration and leakage of the lower units that locally outcrop
540 at the seabed across the ridge. It is also possible that the deep scouring exposed above
541 contributes to the mixing of the bioclastic sands and allows them to rise from the lower units.
542 The absence of bioclastic sands younger than 2,748 cal years B.P. suggests that the sand
543 ridge and proximal dune fields correspond to a fossilized sand reservoir reworked by tidal
544 and wave dynamics. Even if this result needs to be confirmed by complementary data, two

545 hypotheses can be put forth to explain the absence of recent bioclastic sands. First, the
546 absence could be linked to a relative collapse of biological productivity around 3,000 years
547 B.P. Indeed, in contrast to the Holocene transgression that progressively reached the hard
548 floor of the present coast around 7,000 years B.P. and triggered the production of epifauna
549 (Bouysse et al., 1979; Larssonneur et al., 1982), a change in climatic and oceanographic
550 regimes occurring around 3,000 years B.P. is sufficient to explain the absence of recent
551 shells. It matches with the cooling in the NE Atlantic from a significant Arctic glacier event fol-
552 lowing the Minoan Thermal Optimum (Denton and Karlén, 1973; Nesje et al., 2008; Van
553 Vliet-Lanoë et al., 2014b). In a second hypothesis, the absence of recent shells could be
554 induced by the non-conservation of deposits. The age of 3,000 years B.P. also matches with
555 the timing of the beginning of storminess maxima records along the two coastal sedimentary
556 systems of the Seine Estuary and Mont-Saint-Michel Bay located along the southern coast of
557 the English Channel in northwestern France (Sorrel et al., 2012). These events are also
558 recorded by the onset of coastal barrier degradation from 2,400 years B.P. in the Bay of
559 Audierne along SW Brittany (Van Vliet-Lanoë et al., 2014a), and from 4,300 years B.P. in
560 other coastal environments in north and northwest Europe (Sorrel et al., 2012). These
561 modifications would have been sufficient to drive the non-conservation of recent deposits.

562 6.3. Morphologic control

563 The few available dates allow us to somewhat constrain the timing of the building of the
564 *Banc du Four*, and we find that ridge growth was mainly accomplished during the last
565 deglaciation and sea level rise. An older age can not reasonably be presumed, indeed if the
566 preservation of previously emerged bedforms could be considered to occur by early
567 diagenetic cementation, the seismic records should display a pronounced contrast in
568 impedance between the old ridge core made of preserved calcarenites at the base of more
569 recent biogenic sands. This is not observed and the *Banc du Four* is thus assumed to be
570 transgressive in origin. The progressive flooding of the crystalline basement and sills
571 bounding the present location of the sand ridge has induced drastic modifications in this

572 hydrodynamic setting. Consideration of the seismic stratigraphy and morphology of the
573 seafloor basement, together with the ages of the sea-level fluctuations during the Holocene,
574 enables us to suggest an evolutionary scenario for the *Banc du Four* (Fig. 15). The Holocene
575 sea-level change along the French Atlantic and southern English coast continues to be a
576 matter of debate in regards to the response of the continental crust to glacio- and hydro-
577 isostatic effects and regional subsidence, but also regarding the interpretation of coastal
578 markers and palaeo-shorelines as storm deposits (Wingfield, 1995; Lambeck, 1997;
579 Flemming, 1998; Leorri et al., 2012; Goslin et al., 2013). Nevertheless, the recent physical
580 models (Flemming, 1998) do not indicate a significant difference with respect to global sea-
581 level curves (Waelbroeck et al., 2002; Alley et al., 2005; Deschamps et al., 2012). We have
582 thus considered these last reconstructions, except for the last 8 ka for which we have also
583 used the recent local curve of Goslin et al. (2013) that updates the Western Brittany
584 Holocene relative sea-level data. This reconstruction is based on basal peat and compaction-
585 free deposits that have accumulated on top of the Pleistocene formations along Western
586 Brittany, which were recovered during the early-Holocene stages of the post-glacial
587 transgression.

588 According to these studies, the first building stage of the ridge corresponding to the
589 deposits of unit U_{B1} probably started at about 14,000 ($\pm 1,000$) years B.P., when the sea level
590 reached the basement of the ridge at 90 m b.s.l. All of the straits and channels bounding the
591 present ridge had emerged by this time and the first deposits settled in a wide shallow bay
592 open to the northwest. This environment supports the interpretation of the basal unit U_{B1} as
593 shoreface deposits.

594 The depths of the preserved part of unit U_{B2} range between 88 and 60 m b.s.l. The unit
595 was formed by large to giant dunes that imply a water depth of 60 m to 45 m (see above
596 §5.2). This paleobathymetry implies that the SSW-NNE ridge U_{B2} started to grow when the
597 Fromveur strait located west of the ridge, and which is lined up with the U_{B2} ridge, was
598 flooded (Fig. 15). It explains the change in the internal structure of the ridge that records a

599 dominant progradation northward. The rock basement located to the south of the ridge
600 remains emerged.

601 The geometry of the U_{B3} unit, ranging between 90 and 55 m b.s.l., reveals another
602 significant change in the hydrodynamics of the area. New giant tidal dunes rise onto the
603 previous ridge core to the west, and with the exception of small scale fluctuations, the
604 directions of migration are south-westward to the west and northeastward to the east. This
605 apparent residual tidal circulation is similar to present day hydrodynamics across the *Banc*
606 *du Four* and the Ushant-Molene Archipelago. It suggests that the coastline was close to its
607 present location during the formation of U_{B3} . One may also note that U_{B2} is eroded along the
608 eastern flank of the ridge. This can be interpreted as the consequence of the advent of a new
609 pattern of tidal currents including a residual northward trending flow along the eastern edge
610 of the ridge. It correlates with the opening of the Four strait located south of the ridge, where
611 the basal depth is 13 m b.s.l. These elements combine to place the formation of U_{B3} after
612 8,000 (\pm 500) years B.P. with reference to the sea-level curve. It is comparable with the
613 oldest deposits recovered at the top of the shelly sands (7,300 cal years B.P.). Moreover, the
614 interpretation of the U_{B2} and U_{B3} units linked to the flooding of the straits suggests
615 considering them as a kind of tidal deltaic sedimentation due to deceleration of flow at the
616 outlets of the straits; nevertheless, the orientations of net sand transport in both lithosomes
617 are not compatible with deltaic lobe-shaped deposits.

618 The relation of the upper units U_{B4} to U_{B5} to flooding steps are not so obvious, even if
619 the last flooding stages of the shallow minor sills (maximum depths 6 m b.s.l.) surrounding
620 the Molene Archipelago could have modified local tidal currents. However, the geometries of
621 units do not lined up with the numerous orientations of the sills (Fig. 5). The stages from U_{B3}
622 to U_{B5} are probably more gradational, corresponding to an overall extension of the ridge to
623 the west, where it enters in the increasing influence of the tidal gyre of the Ushant Island. In
624 this way, U_{B4} could be the stratigraphic expression of the dune intergroup area preserved at
625 the same place and visible in the modern bathymetric map. The superimposed units U_{B3} to
626 U_{B5} , and major bounding surfaces R_{B3} and R_{B4} , would thus predominantly be produced by an

627 autocyclic process of sand ridge development. Such an interpretation has been made for the
628 internal architecture of tidal sand ridges in the East China Sea (Liu et al., 2007).

629 However, external parameters as storm waves may also have partially contributed to
630 shape the bounding surfaces. The flattened top of the U_{B5} blanket-shaped (Line 13-14, Fig. 3)
631 is effectively exposed to storm waves as shown by the comparison of recent swath
632 bathymetric surveys (Franzetti et al., 2013).

633 7. Conclusion

634 The seismic survey of the *Banc du Four* located offshore Brittany enabled us to
635 characterize the long-term evolution and internal architecture of this deep tidal ridge.

636 Five seismic units have been distinguished within the ridge, separated by major
637 bounding surfaces and revealing that the ridge construction evolved in stages. The ridge
638 growth was made possible by the presence of a nucleus forming a juvenile ridge interpreted
639 as shoreface deposits. They progressively grade upwards to offshore deposits composed of
640 large-scale tidal dunes. Sandwave climbing, which combines progradation and accretion, is
641 the major process controlling the growth of the ridge. The elevation of the preserved dune
642 foresets reaches values of about 20 to 30 m within the ridge and indicates a combination of
643 giant dunes characterized by numerous steep (until 20°) clinoforms that denote a high-
644 energy depositional environment. Moreover, the presence of scour pits linked to the 3D
645 geometries of giant dunes allow the growth of bedforms migrating oblique to the orientation
646 of the giant dune crest lines. All of the radiocarbon ages of the biogenic surficial deposits of
647 the *Banc du Four* range from 10,036 to 2,748 cal years B.P. and suggest that the *Banc du*
648 *Four* has grown during the last sea-level rise, as well its morphology reveals it is still active.
649 Moreover, the long-term evolution of the ridge appears strongly controlled by the morphology
650 of the igneous basement. The multiphase accretion of the ridge is closely linked to the
651 presence of a residual tidal current eddy, subsequent to the progressive flooding of the
652 coastal promontories and straits that structured the igneous basement.

653 The *Banc du Four* is thus representative of an evolved stage of tidal sand ridge, and is
654 still active. It should be referred to as representative of a large-scale high-energy banner
655 bank where large and steep clinoforms are depicted in a modern environment.

656 8. Acknowledgments

657 We wish first to thank Pr. Serge Berné and Pr. Jean-Yves Reynaud for their careful
658 reviewing and constructive comments.

659 This work was funded by the Direction Générale de l'Armement (DGA) and the SHOM.
660 This project also benefits from the support of the Labex Mer (ANR-10-LABX-19-01, IUEM,
661 Brest). We are very grateful to the crews of the vessels “Pourquoi-Pas?”, “Côtes de la
662 Manche” and “Albert Lucas” (Daniel Morigeon and Franck Quéré), and also thank the
663 scientists and technicians for their participation in the project and the cruise: B Van Vliet
664 Lanoë, C. Prunier and A. Deschamps. We are also grateful to the improvement of the
665 English version by Katalin Kovacs (Services de Relecture Scientifique,
666 astronogirl@gmail.com).

667

668 Allen, J.R.L., 1970. A quantitative model of climbing ripples and their
669 crosslaminated deposits. *Sedimentology* 14, 5–26. doi:10.1111/j.1365-
670 3091.1970.tb00179.x

671 Alley, R.B., Dupont, T.K., Parizek, B.R., Anandakrishnan, S., 2005. Access of
672 surface meltwater to beds of sub-freezing glaciers: preliminary insights. *Ann. Glaciol.*
673 40, 8–14. doi:10.3189/172756405781813483

674 Andreieff, P., Bouysse, P., Horn, R., Monciardini, C., 1972. Contribution à
675 l'étude géologique des approches occidentales de la Manche. *Mém. Bur. Rech.*
676 *Géologiques Minières* 79, 32–48.

677 Auffret, G.A., 1983. Dynamique sédimentaire de la marge continentale celtique
678 - Evolution Cénozoïque - Spécificité du Pleistocène supérieur et de l'Holocène
679 (Docteur). Université de Bordeaux I, Bordeaux, France.

680 Auffret, J.-P., Alduc, D., Larsonneur, C., Smith, A.J., 1980. Cartographie du
681 réseau des paléo- vallées et de l'épaisseur des formations superficielles meubles de
682 la Manche orientale. *Ann. Inst. Océan.* 56, 21–35.

683 Bastos, A., Collins, M.B., Kenyon, N.H., 2003. Water and sediment movement
684 around a coastal headland: Portland Bill, southern UK. *Ocean Dyn.* 53, 309–321.
685 doi:10.1007/s10236-003-0031-1

686 Belderson, R.H., Johnson, M.A., Kenyon, N.H., 1982. Bedforms, in: Stride, A.H.
687 (Ed.), *Offshore Tidal Sands : Processes and Deposits*. London ; New York, pp. 27–
688 57.

689 Berné, S., 2002. Evolution of sand banks. *Comptes Rendus Geosci.* 334, 731–
690 732.

691 Berné, S., 1999. Dynamique, architecture et préservation des corps sableux de
692 plate-forme (Habilitation à diriger des recherches). Université Lille 1, Lille.

693 Berné, S., Allen, G.P., Auffret, J.-P., Chamley, H., Durand, J., Weber, O., 1989.
694 Essai de synthèse sur les dunes hydrauliques géantes tidales actuelles. Bull. Société
695 Géologique Fr. 6, 1145–1160.

696 Berné, S., Auffret, J.-P., Walker, P., 1988. Internal structure of subtidal
697 sandwaves revealed by high-resolution seismic reflection. Sedimentology 35, 5–20.
698 doi:10.1111/j.1365-3091.1988.tb00902.x

699 Berné, S., Castaing, P., Le Drezen, E., Lericolais, G., 1993. Morphology,
700 Internal Structure, and Reversal of Asymmetry of Large Subtidal Dunes in the
701 Entrance to Gironde Estuary (France). J. Sediment. Res. 63, 780–793.
702 doi:10.1306/D4267C03-2B26-11D7-8648000102C1865D

703 Berné, S., Lericolais, G., Marsset, T., Bourillet, J.-F., De Batist, M., 1998.
704 Erosional offshore sand ridges and lowstand shorfaces : eamples from tide- and
705 wave -dominated environments of France. J. Sediment. Res. 68, 540–555.

706 Berné, S., Trentesaux, A., Stolk, A., Missiaen, T., De Batist, M., 1994.
707 Architecture and long term evolution of a tidal sandbank : The Middelkerke Bank
708 (southern North Sea). Mar. Geol. 121, 57–72.

709 Berné, S., Vagner, P., Guichard, F., Lericolais, G., Liu, Z., Trentesaux, A., Yin,
710 P., Yi, H.I., 2002. Pleistocene forced regressions and tidal sand ridges in the East
711 China Sea. Mar. Geol. 188, 293–315. doi:10.1016/S0025-3227(02)00446-2

712 Berthot, A., Pattiaratchi, C., 2006. Mechanisms for the formation of headland-
713 associated linear sandbanks. Cont. Shelf Res. 26, 987–1004.
714 doi:10.1016/j.csr.2006.03.004

715 Boersma, J.R., 1970. Distinguishing Features of Wave Ripple Cross
716 Stratification and Morphology (Docteur). University of Utrecht, Utrecht, The
717 Netherlands.

718 Bouysse, P., Horn, R., Lefort, J.-P., Le Lann, F., 1975. Tectonique et structures
719 post-paléozoïques en Manche occidentale. *Philos. Trans. R. Soc. Lond.* 279, 41–54.

720 Bouysse, P., Le Lann, F., Scolari, G., 1979. Les sédiments superficiels des
721 Approches occidentales de la Manche. *Mar. Geol.* 29, 107–135. doi:10.1016/0025-
722 3227(79)90105-1

723 Brookfield, M.E., 1977. The origin of bounding surfaces in ancient aeolian
724 sandstones. *Sedimentology* 24, 303–332. doi:10.1111/j.1365-3091.1977.tb00126.x

725 Cameron, T.D.J., Crosby, A., Balson, P.S., Jeffrey, D.H., Lott, G.K., Bulat, J.,
726 Harrison, D.J., 1992. United Kingdom offshore regional report: the geology of the
727 southern North Sea, HMSO for the British Geological Survey. London.

728 Chaumillon, E., Tessier, B., Reynaud, J.-Y., 2011. Variability of Incised Valleys
729 and Estuaries Along French Coasts: An Analog to Oil Reservoirs Where Topography
730 Influence Preservation Potential? Presented at the 2011 CSPG CSEG CWLS
731 Convention, Calgary (Canada), pp. 1–4.

732 Dalrymple, R.W., Rhodes, R.N., 1995. Chapter 13 Estuarine Dunes and Bars,
733 in: *Developments in Sedimentology*. Elsevier, pp. 359–422.

734 Davies, P.A., Dakin, J.M., Falconer, R.A., 1995. Eddy Formation behind a
735 Coastal Headland. *J. Coast. Res.* 11, 154–167.

736 Davis, R.A., Balson, P.S., 1992. Stratigraphy of a North Sea Tidal Sand Ridge.
737 *J. Sediment. Petrol.* 62, 116–121.

738 Dehouck, A., 2006. Observations et conditions d'apparition des croissants de
739 plage sur le littoral de la mer d'Iroise. *Noréis* 7–16. doi:10.4000/noréis.1732

740 Deleu, S., Van Lancker, V., Van den Eynde, D., Moerkerke, G., 2004.
741 Morphodynamic evolution of the kink of an offshore tidal sandbank: the Westhinder
742 Bank (Southern North Sea). *Cont. Shelf Res.* 24, 1587–1610.

743 doi:10.1016/j.csr.2004.07.001

744 Denton, G.H., Karlén, W., 1973. Holocene Climatic Variations - Their Pattern
745 and Possible Cause. *Quat. Res.* 155–205.

746 Deschamps, P., Durand, N., Bard, E., Hamelin, B., Camoin, G., Thomas, A.L.,
747 Henderson, G.M., Okuno, J., Yokoyama, Y., 2012. Ice-sheet collapse and sea-level
748 rise at the Bølling warming 14,600 years ago. *Nature* 483, 559–564.
749 doi:10.1038/nature10902

750 D'Olier, B., 1981. Sedimentary Events during Flandrian Sea-Level Rise in the
751 South-West Corner of the North Sea. *Int. Assoc. Sedimentol., Special Publication*
752 221–227.

753 Dyer, K.R., Huntley, D.A., 1999. The origin, classification and modelling of sand
754 banks and ridges. *Cont. Shelf Res.* 19, 1285–1330. doi:10.1016/S0278-
755 4343(99)00028-X

756 Evans, C.D.R., 1990. The geology of the western English Channel and its
757 western approaches, United Kingdom Offshore Regional Report. HMSO, London.

758 Ferret, Y., Le Bot, S., Tessier, B., Garlan, T., Lafite, R., 2010. Migration and
759 internal architecture of marine dunes in the eastern English Channel over 14 and 56
760 year intervals: the influence of tides and decennial storms. *Earth Surf. Process.*
761 *Landf.* 35, 1480–1493. doi:10.1002/esp.2051

762 Flemming, N.C., 1998. Archaeological evidence for vertical movement on the
763 continental shelf during the Palaeolithic, Neolithic and Bronze Age periods. *Geol.*
764 *Soc. Lodon, Special Publications* 146, 129–146.
765 doi:10.1144/GSL.SP.1999.146.01.07

766 Folk, R.L., Ward, W.C., 1957. Brazos River bar : a study in the significance of
767 grain size parameters. *J. Sediment. Res.* 27, 3–26.

768 Franzetti, M., 2014. Dynamique des bancs et dunes sableuses de plateforme
769 en contexte macrotidal : l'exemple du Banc du Four (Ouest Bretagne) (Docteur).
770 Université de Bretagne Occidentale, Brest, France.

771 Franzetti, M., Le Roy, P., Delacourt, C., Garlan, T., Cancouët, R., Sukhovich,
772 A., Deschamps, A., 2013. Giant dune morphologies and dynamics in a deep
773 continental shelf environment: Example of the Banc du Four (Western Brittany,
774 France). *Mar. Geol.* 346, 17–30. doi:10.1016/j.margeo.2013.07.014

775 Goslin, J., Van Vliet-Lanoë, B., Stephan, P., Delacourt, C., Fernane, A.,
776 Gandouin, E., Hénaff, A., Penaud, A., Suanez, S., 2013. Holocene relative sea-level
777 changes in western Brittany (France) between 7600 and 400 cal. B.P. :
778 Reconstruction from basal-peat deposits. *Géomorphologie Relief Process. Environ.*
779 4, 54–72.

780 Guillou, N., 2007. Rôles de l'hétérogénéité des sédiments de fond et des
781 interactions houle-courant sur l'hydrodynamique et la dynamique sédimentaire en
782 zone subtidale - applications en Manche orientale et à la pointe de la Bretagne
783 (Docteur). Université de Bretagne Occidentale, Brest, France.

784 Hirschberger, F., 1970. L'Iroise et les abords d'Ouessant et de Sein,
785 Association des Publications de la Faculté des Lettres et Sciences Humaines.
786 Université de Caen, Caen.

787 Hirschberger, F., 1962a. Résultats de 14 stations hydrologiques dans l'iroise et
788 à ses abords. *Académie Sci.* 2628–2631.

789 Hirschberger, F., 1962b. Les hauts fonds sableux de l'iroise et leurs rapports
790 avec les courants de marée. *Ibidem* 74, 53–80.

791 Hommeril, P., 1971. Datation absolue de sédiments bioclastiques provenant
792 des bancs sous-marin du golfe normand-breton. *Comptes Rendus Somm. Séances*

793 Société Géologique Fr. 112–113.

794 Houbolt, J.J.H., 1968. Recent sediments in the southern Bight of the North
795 Sea, *Geologie en Mijnbouw*.

796 Huthnance, J.M., 1982a. On the formation of sand banks of finite extent. *Estuar.
797 Coast. Shelf Sci.* 15, 277–299. doi:10.1016/0272-7714(82)90064-6

798 Huthnance, J.M., 1982b. On one mechanism forming linear sand banks. *Estuar.
799 Coast. Shelf Sci.* 14, 79–99. doi:10.1016/S0302-3524(82)80068-6

800 Huthnance, J.M., 1973. Tidal current asymmetries over the Norfolk Sandbanks.
801 *Estuar. Coast. Mar. Sci.* 1, 89–99. doi:10.1016/0302-3524(73)90061-3

802 Jelgersma, S., 1979. Sea-level changes in the North Sea basin. In *The
803 Quaternary History of the North Sea*, in: Oele, E., Schüttenhelm, R.T.E., Wiggers,
804 A.J. (Eds.), . Presented at the Symposia Universitatis Upsaliensis annum
805 quingentesimum celebrantis 2, pp. 233–248.

806 Jin, J.H., Chough, S.K., 2002. Erosional shelf ridges in the mid-eastern Yellow
807 Sea. *Geo-Mar. Lett.* 21, 219–225. doi:10.1007/s00367-001-0082-6

808 Jopling, A.V., Walker, R.G., 1968. Morphology and Origin of Ripple-Drift Cross-
809 Lamination, with Examples from the Pleistocene of Massachusetts. *SEPM J.
810 Sediment. Res.* 38, 971–984. doi:10.1306/74D71ADC-2B21-11D7-
811 8648000102C1865D

812 Jung, W.Y., Suk, B.C., Min, G.H., Lee, Y.K., 1998. Sedimentary structure and
813 origin of a mud-cored pseudo-tidal sand ridge, eastern Yellow Sea, Korea. *Mar. Geol.*
814 151, 73–88. doi:10.1016/S0025-3227(98)00058-9

815 Kenyon, N.H., Belderson, R.H., Stride, A.H., Johnson, M.A., 1981. Offshore
816 Tidal Sand-Banks as Indicators of Net Sand Transport and as Potential Deposits, in:
817 Nio, S.-D., Shüttenhelm, R.T.E., Van Weering, T.C.E. (Eds.), *Holocene Marine*

818 Sedimentation in the North Sea Basin. Blackwell Scientific Publications, Oxford, UK,
819 pp. 257–268.

820 Kenyon, N.H., Cooper, B., 2005. Sand banks sand transport and offshore wind
821 farms, DTI commissioned report.

822 Kenyon, N.H., Stride, A.H., 1970. The tide-swept continental shelf sediments
823 between the Shetland Isles and France. *Sedimentology* 14, 159–173.
824 doi:10.1111/j.1365-3091.1970.tb00190.x

825 Laban, C., Schüttenhelm, R.T.E., 1981. Some New Evidence on the Origin of
826 the Zeeland Ridges. *Int. Assoc. Sedimentol., Special Publication* 239–245.

827 Lambeck, K., 1997. Sea-level change along the French Atlantic and Channel
828 coasts since the time of the Last Glacial Maximum. *Palaeogeogr. Palaeoclimatol.*
829 *Palaeoecol.* 129, 1–22. doi:10.1016/S0031-0182(96)00061-2

830 Lapierre, F., Bouysse, P., 1975. Carte géologique de la marge continentale
831 française à l'échelle du 1/250000 Ouessant.

832 Larsonneur, C., Bouysse, P., Auffret, J.-P., 1982. The superficial sediments of
833 the English Channel and its Western Approaches. *Sedimentology* 29, 851–864.
834 doi:10.1111/j.1365-3091.1982.tb00088.x

835 Le Bot, S., 2001. Morphodynamique de dunes sous-marines sous influence des
836 marées et des tempêtes : processus hydro-sédimentaires et enregistrement
837 exemple du Pas-de-Calais (Docteur). Université Lille 1, Lille.

838 Le Bot, S., Trentesaux, A., 2004. Types of internal structure and external
839 morphology of submarine dunes under the influence of tide- and wind-driven
840 processes (Dover Strait, northern France). *Mar. Geol.* 211, 143–168.
841 doi:10.1016/j.margeo.2004.07.002

842 Leorri, E., Cearreta, A., Milne, G., 2012. Field observations and modelling of

843 Holocene sea-level changes in the southern Bay of Biscay: implication for
844 understanding current rates of relative sea-level change and vertical land motion
845 along the Atlantic coast of SW Europe. *Quat. Sci. Rev.* 42, 59–73.
846 doi:10.1016/j.quascirev.2012.03.014

847 Le Roy, P., Gracia-Garay, C., Guennoc, P., Bourillet, J.-F., Reynaud, J.-Y.,
848 Thinon, I., Kervevan, P., Paquet, F., Menier, D., Bulois, C., 2011. Cenozoic tectonics
849 of the Western Approaches Channel basins and its control of local drainage systems.
850 *Bull. Soc. Geol. Fr.* 182, 451–463. doi:10.2113/gssgfbull.182.5.451

851 Liu, Z., Berné, S., Saito, Y., Yu, H., Trentesaux, A., Uehara, K., Yin, P., Paul
852 Liu, J., Li, C., Hu, G., Wang, X., 2007. Internal architecture and mobility of tidal sand
853 ridges in the East China Sea. *Cont. Shelf Res.* 27, 1820–1834.
854 doi:10.1016/j.csr.2007.03.002

855 Marsset, T., Tessier, B., Reynaud, J.-Y., De Batist, M., Plagnol, C., 1999. The
856 Celtic Sea banks: an example of sand body analysis from very high-resolution
857 seismic data. *Mar. Geol.* 158, 89–109. doi:10.1016/S0025-3227(98)00188-1

858 Meene, J.W.H. van de, 1994. The shoreface-connected ridges along the central
859 Dutch coast (Docteur). Koninklijk Nederlands Aardrijkskundig Genootschap/Faculteit
860 Ruimtelijke Wetenschappen, Universiteit Utrecht, Utrecht.

861 M'Hammdi, N., 1994. Architecture du banc sableux tidal de Serq (Iles anglo-
862 normandes) (Docteur). Université Lille 1, Lille.

863 M'Hammdi, N., Berné, S., Bourillet, J.-F., Auffret, J.-P., 1992. Architecture of a
864 tidal sand bank : the Shark Bank (Channel Islands), in: Flemming, B.W. (Ed.),
865 *Modern and Ancient Clastic Tidal Deposits*. pp. 59–60.

866 Neill, S.P., Scourse, J.D., 2009. The formation of headland/island sandbanks.
867 *Cont. Shelf Res.* 29, 2167–2177. doi:10.1016/j.csr.2009.08.008

868 Nesje, A., Dahl, S.O., Thun, T., Nordli, Ø., 2008. The “Little Ice Age” glacial
869 expansion in western Scandinavia: summer temperature or winter precipitation?
870 *Clim. Dyn.* 30, 789–801. doi:10.1007/s00382-007-0324-z

871 Olariu, C., Steel, R.J., Dalrymple, R.W., Gingras, M.K., 2012. Tidal dunes
872 versus tidal bars: The sedimentological and architectural characteristics of compound
873 dunes in a tidal seaway, the lower Baronia Sandstone (Lower Eocene), Ager Basin,
874 Spain. *Sediment. Geol.* 279, 134–155. doi:10.1016/j.sedgeo.2012.07.018

875 Quesney, A., 1983. Manche occidentale et mer Celtique. Etude des
876 paléovallées, des fosses et des formations superficielles. (Docteur). Université de
877 Caen, Caen, France.

878 Raffin, C., 2003. Bases biologiques et écologiques de la conservation du milieu
879 marin en mer d'Iroise (Docteur). Université de Bretagne Occidentale, Brest, France.

880 Reimer, P.J., Baillie, M.G., Bard, E., Bayliss, A., Beck, J.W., Blackwell, P.G.,
881 Bronk Ramsey, C., Buck, C.E., Burr, G.S., Edwards, R.L., Friedrich, M., Grootes,
882 P.M., Guilderson, T.P., Hajdas, I., Heaton, T.J., Hogg, A.G., Hughen, K.A., Kaiser,
883 K.F., Kromer, B., McCormac, F.G., Manning, S.W., Reimer, R.W., Richards, D.A.,
884 Southon, J.R., Talamo, S., Turney, C.S.M., Van Der Plicht, J., Weyhenmeyer, C.E.,
885 2009. IntCal09 and Marine09 Radiocarbon Age Calibration Curves, 0-50,000 Years
886 cal BP. *Radiocarbon* 51, 1111–1150.

887 Reynaud, J.-Y., 1996. Architecture et évolution d'un banc sableux de mer
888 celtique méridionale (Docteur). Université Lille 1, Lille.

889 Reynaud, J.-Y., Dalrymple, R.W., 2012. Shallow-Marine Tidal Deposits, in:
890 Davis, R.A., Dalrymple, R.W. (Eds.), *Principles of Tidal Sedimentology*. Springer
891 Netherlands, Dordrecht, pp. 335–369.

892 Reynaud, J.-Y., Tessier, B., Auffret, J.-P., Berné, S., De Batist, M., Marsset, T.,

893 Walker, P., 2003. The offshore Quaternary sediment bodies of the English Channel
894 and its Western Approaches. *J. Quat. Sci.* 18, 361–371. doi:10.1002/jqs.758

895 Reynaud, J.-Y., Tessier, B., Berné, S., Chamley, H., De Batist, M., 1999a. Tide
896 and wave dynamics on a sand bank from the deep shelf of the Western Channel
897 approaches. *Mar. Geol.* 161, 339–359. doi:10.1016/S0025-3227(99)00033-X

898 Reynaud, J.-Y., Tessier, B., Proust, J.-N., Dalrymple, R.W., Marsset, T., De
899 Batist, M., Bourillet, J.-F., Lericolais, G., 1999b. Eustatic and hydrodynamic controls
900 on the architecture of a deep shelf sand bank (Celtic Sea). *Sedimentology* 46, 703–
901 721. doi:10.1046/j.1365-3091.1999.00244.x

902 Rubin, D.M., 1987. Cross-Bedding, Bedforms, and Paleocurrents, SEPM
903 Society for Sedimentary Geology. ed, *Concepts in Sedimentology and Paleontology*.
904 Oklahoma.

905 Rubin, D.M., Carter, C.L., 2006. Cross-bedding, Bedforms and Paleocurrents,
906 SEPM. ed, *Atlas*.

907 Rubin, D.M., Hunter, R.E., 1982. Bedform climbing in theory and nature.
908 *Sedimentology* 29, 121–138. doi:10.1111/j.1365-3091.1982.tb01714.x

909 Rubin, D.M., Ikeda, H., 1990. Flume experiments on the alignment of
910 transverse, oblique, and longitudinal dunes in directionally varying flows.
911 *Sedimentology* 37, 673–684. doi:10.1111/j.1365-3091.1990.tb00628.x

912 SEPM's Research Conference. 2008. Steel, R., Nittrouer, C. (convenors). *Cliniform*
913 *Sedimentary Deposits: The Processes Producing Them and the Stratigraphy Defining*
914 *Them*. SEPM's Research Conference, 15-18 August 2008, Rock Springs, Wyoming.

915 Snedden, J.W., Dalrymple, R.W., 1999. Modern shelf sand ridges : from
916 historical perspective to a unified hydrodynamic and evolutionary model, in:
917 Bergman, K.M., Snedden, J.W. (Eds.), *Isolated Shallow Marine Sand Bodies :
918 Sequence Stratigraphic Analysis and Sedimentologic Interpretation*, Special

919 Publication. SEPM (Society for Sedimentary Geology), pp. 13–28.

920 Sorrel, P., Debret, M., Billeaud, I., Jaccard, S.L., McManus, J.F., Tessier, B.,
921 2012. Persistent non-solar forcing of Holocene storm dynamics in coastal
922 sedimentary archives. *Nat. Geosci.* 5, 892–896. doi:10.1038/ngeo1619.

923 Tessier, B., 1997. *Expressions Sédimentaires de la Dynamique Tidale*
924 (Habilitation à diriger des recherches). Université Lille 1, Lille.

925 Tessier, B., Billeaud, I., Lesueur, P., 2010. Stratigraphic organisation of a
926 composite macrotidal wedge: the Holocene sedimentary infilling of the Mont-Saint-
927 Michel Bay (NW France). *Bull. Soc. Geol. Fr.* 181, 99–113.
928 doi:10.2113/gssgfbull.181.2.99

929 Trentesaux, A., Stolk, A., Berné, S., 1999. Sedimentology and stratigraphy of a
930 tidal sand bank in the southern North Sea. *Mar. Geol.* 159, 253–272.
931 doi:10.1016/S0025-3227(99)00007-9

932 Uehara, K., Scourse, J.D., Horsburgh, K.J., Lambeck, K., Purcell, A.P., 2006.
933 Tidal evolution of the northwest European shelf seas from the Last Glacial Maximum
934 to the present. *J. Geophys. Res.* 111. doi:10.1029/2006JC003531

935 Van Landeghem, K.J.J., Baas, J.H., Mitchell, N.C., Wilcockson, D., Wheeler,
936 A.J., 2012. Reversed sediment wave migration in the Irish Sea, NW Europe: A
937 reappraisal of the validity of geometry-based predictive modelling and assumptions.
938 *Mar. Geol.* 295-298, 95–112. doi:10.1016/j.margeo.2011.12.004

939 Van Veen, J., 1936. *Nieuwe Verhandelingen van het Bataafsch Genootschap*
940 *der proefondervindelijke wijsbegeerte te Rotterdam* (No. 11), 12. Gravenhage
941 ministerie van waterstaat.

942 Van Vliet-Lanoë, B., Goslin, J., Hallégouët, B., Hénaff, A., Delacourt, C.,
943 Fernane, A., Franzetti, M., Le Cornec, E., Le Roy, P., Penaud, A., 2014a. Middle- to

944 late-Holocene storminess in Brittany (NW France): Part I - morphological impact and
945 stratigraphical record. *The Holocene*. doi:10.1177/0959683613519687

946 Van Vliet-Lanoë, B., Penaud, A., Hénaff, A., Delacourt, C., Fernane, A., Goslin,
947 J., Hallégouët, B., Le Cornec, E., 2014b. Middle- to late-Holocene storminess in
948 Brittany (NW France): Part II - The chronology of events and climate forcing. *The*
949 *Holocene*. doi:10.1177/0959683613519688

950 Vecchi, L.G., Aliotta, S., Ginsberg, S.S., Giagante, D.A., 2013. Morphodynamic
951 behavior and seismostratigraphy of a sandbank: Bahía Blanca estuary, Argentina.
952 *Geomorphology* 189, 1–11. doi:10.1016/j.geomorph.2013.01.003

953 Waelbroeck, C., Labeyrie, L., Michel, E., Duplessy, J.C., McManus, J.F.,
954 Lambeck, K., Balbon, E., Labracherie, M., 2002. Sea-level and deep water
955 temperature changes derived from benthic foraminifera isotopic records. *Quat. Sci.*
956 *Rev.* 21, 295–305. doi:10.1016/S0277-3791(01)00101-9

957 Walker, P., 2001. Dynamique sédimentaire dans le golfe normand-breton :
958 intérêt de l'imagerie par sonar à balayage latéral (Docteur). Université de Caen /
959 Basse Normandie, Caen, France.

960 Wilson, J.B., 1982. Shelly faunas associated with temperate offshore tidal
961 deposits, in: *Offshore Tidal Sands*. Springer Netherlands, Dordrecht, pp. 126–171.

962 Wingfield, R.T.R., 1995. A model of sea levels in the Irish and Celtic Seas
963 during the End Pleistocene to Holocene transition, in: *Island Britain : A Quaternary*
964 *Perspective*. pp. 181–208.

965 Wolanski, E., Imberger, J., Heron, M., 1984. Island wakes in coastal waters. *J.*
966 *Geophys. Res.* 89, 553–569.

967 Yalin, M.S., 1964. Geometrical properties of sand waves. *J. Hydraul.* 90, 105–
968 119.

969 Yang, C.-S., Sun, J.-S., 1988. Tidal sand ridges on the East China Sea shelf, in:
970 De Boer, P.L., Van Gelder, A., Nio, S.-D. (Eds.), *Tide : Influenced Sedimentary*
971 *Environments and Facies*. pp. 23–38.

972

973 Table 1. Radiocarbon datations of the surficial deposits of the Banc du Four.
974 Calibrations yield ages with 1 standard deviation. We applied a regional deviation ΔR of $-40 \pm$
975 42 years corresponding to the nearby Sein Island (Marine reservoir correction database:
976 <http://intcal.qub.ac.uk/marine/>).

977

978 Figure 1. (A) Map of the Iroise sea (situated between the French Brittany coast and the
979 Ushant-Molene Archipelago), showing the location of the *Banc du Four* (from the DTM
980 acquired during the EvalHydro 2009 survey). This ridge system is defined by offshore
981 bedforms which define a V shape. The water depth of the basement ranges from 70 to 105 m
982 below Lower Astronomical Tide. (B) Eulerian residual tidal currents and maximum shear
983 velocities at seabed according to the French Coastal Oceanographic Centre (Previmer) for a
984 tidal range of 90. Pecked lines are co-range lines joining points of the same tidal range.

985

986 Figure 2. (A) Detailed view of the *Banc du Four* system with crest heights and migration
987 rates. From Franzetti et al. (2013). (B) Bathymetry of the Banc du Four from DTM 2009 with
988 locations of the Shipeck grab samples. There are two types of sediment on the ridge system:
989 type 1 is composed of medium to coarse bioclastic sands, while type 2 is characterized by
990 siliciclastic gravels.

991

992 Figure 3. A: Location of the sparker seismic lines used in this study. B: Interpretative
993 line drawings of several representative seismic lines. C: Extracts of representative seismic
994 lines corresponding to selected sections of previous line drawings (location on Fig. 3B).

995 Three seismic units (U_{S1} to U_{S3}) are distinguished within the substratum and five within the
996 ridge (U_{B1} to U_{B5}).

997

998 Figure 4. Spatial extension of the ridge's seismic units merging at seabed and
999 correlation with the surficial sediments. Locations of the samples with radiocarbon datations
1000 (ages cal years B.P.). See Tab.1 for details.

1001

1002 Figure 5. Isopach maps (in ms TWT two way travel time) of the ridge seismic units U_{B1}
1003 to U_{B5} . The present ridge system has been removed from the bathymetric DTM shown
1004 backward and only its outline is shown (black line, insert up left). The polylines correspond to
1005 the extension of the interpolation areas.

1006

1007 Figure 6. Extract and interpretative line drawing of the seismic line 12-03 showing the
1008 geometry of the U_{S3} substratum seismic unit. It is interpreted as the infilling of a fluvial paleo-
1009 valley incised at the top of the Neogene basin (U_{S2}).

1010

1011 Figure 7. Extension of the Neogene basin corresponding to the substratum seismic unit
1012 U_{S2} (orange line). The geometry of the structure, bounded by northwestward-dipping normal
1013 faults (red lines), delineates a faulted block (modified from Gallais et al., 2007 and Le Gall et
1014 al., 2015). In blue : reconstruction of the probable paleovalley network around the *Banc du*
1015 *Four* drawn from the morphology of the crystalline basement and extension of the U_{S3}
1016 seismic unit.

1017

1018 Figure 8. Extract and interpretative line drawing of seismic line 12-03 showing the
1019 geometry of the U_{B1} ridge seismic unit. The location corresponds to the solid black line. The
1020 internal reflectors are sub-horizontal to the south, and grade to northwestward gently-dipping
1021 clinoforms to the north.

1022

1023 Figure 9. Extract and interpretative line drawing of the seismic line 12-09 showing the
1024 geometry of the U_{B2} ridge seismic unit.

1025

1026 Figure 10. Extracts and interpretative line drawing of seismic line 13-07 showing the
1027 geometry of the U_{B3} ridge seismic unit. The unit is composed of superimposed sets with the
1028 geometry of the reflectors consisting of oblique-parallel to oblique-tangential profiles. It is
1029 interpreted as corresponding to large climbing dunes with no stoss-side preservation.

1030

1031 Figure 11. Extracts and interpretative line drawing of seismic line 13-14 showing the
1032 geometry of the U_{B4} ridge seismic unit. The unit is characterized by large and slightly oblique
1033 clinofolds. The reflectors are considered to be formed by lateral accretion of the ridge
1034 surface.

1035

1036 Figure 12. Extracts and interpretative line drawings of the two secant seismic lines 13-
1037 06 and 12-08, showing the geometry of the U_{B5} ridge seismic unit. The geometry of the unit is
1038 characterized by a succession of aggrading and prograding climbing sets of reflectors. They
1039 are interpreted as massive climbing dunes.

1040

1041 Figure 13. Extract and interpretative line drawing of seismic line 13-08 showing the
1042 presence of large concave-up geometries within the U_{B3} ridge seismic unit.

1043

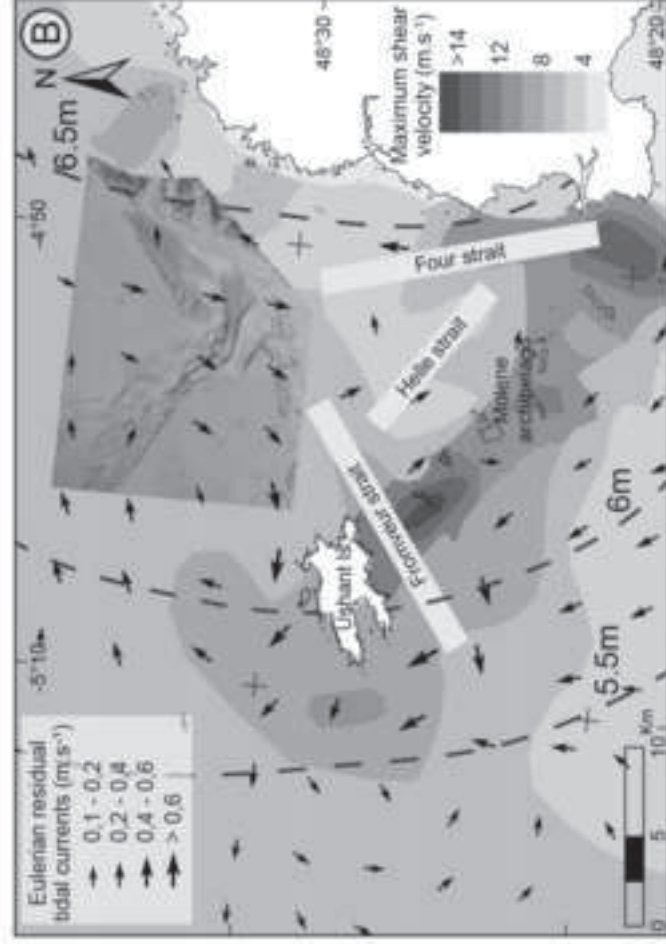
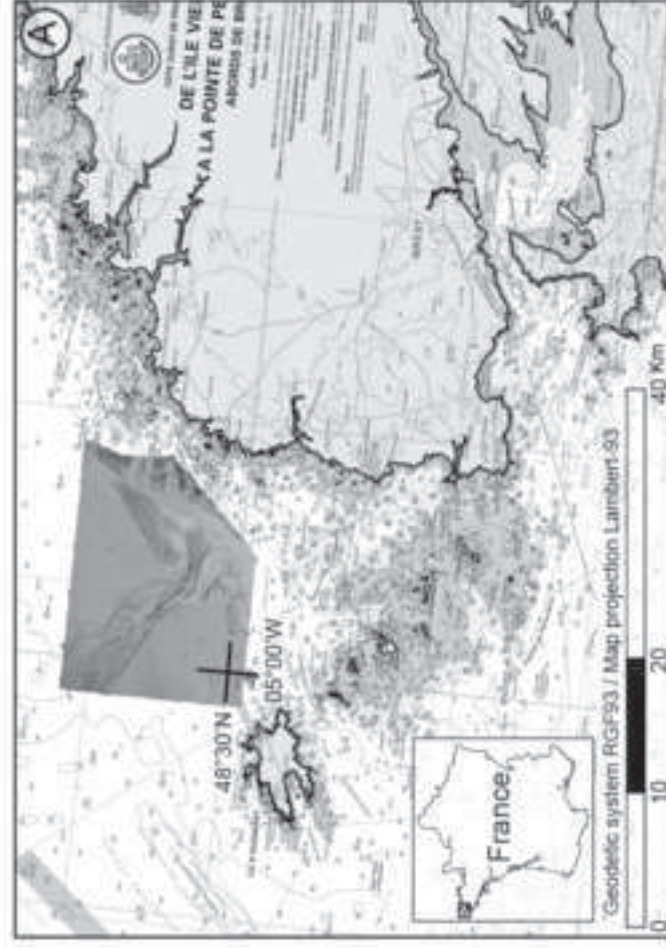
1044 Figure 14. Bathymetry map (Daurade 2010 survey) of the western border of the *Banc*
1045 *du Four* and corresponding 3D view showing the internal geometry of the U_{B5} seismic unit
1046 through extracts 12-08 and 13-04. It shows the succession of scour pits between giant
1047 dunes. The deposits have been removed within the troughs. White arrows represent the
1048 direction of dune migrations deduced from the asymmetry of the bedforms. Red arrows
1049 represent deduced orientations of erosive currents.

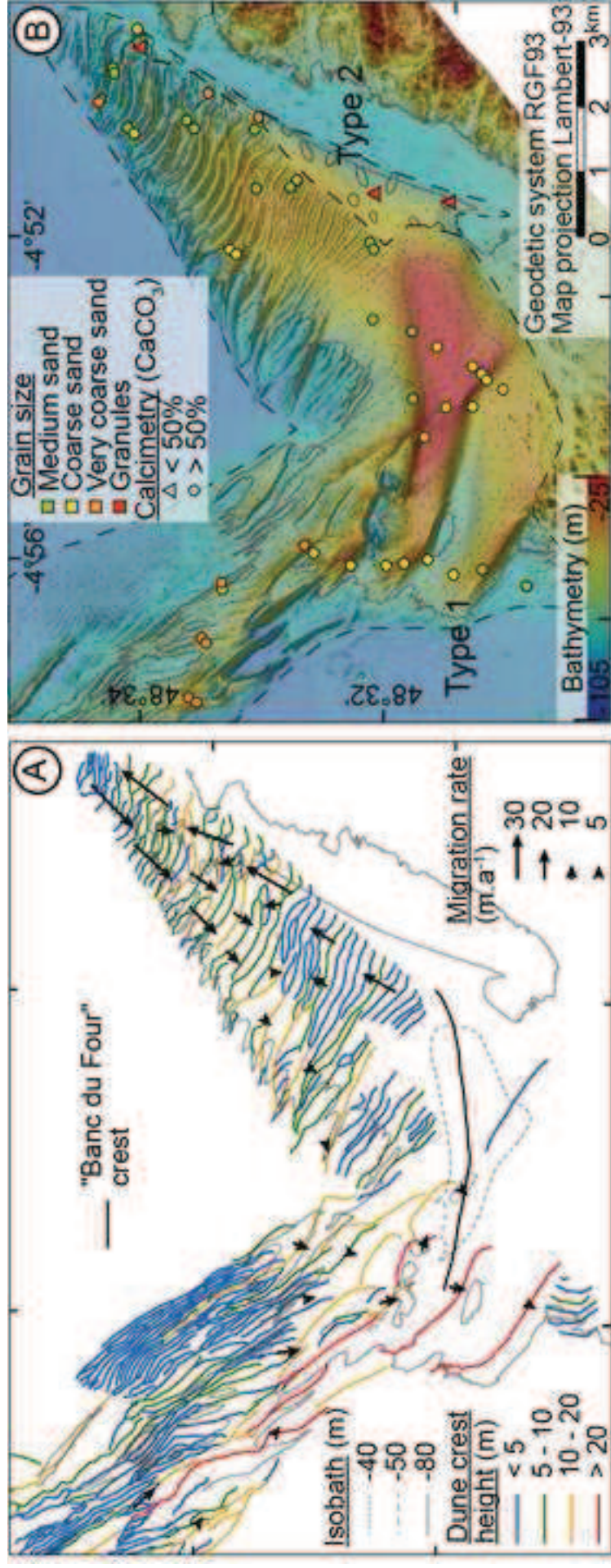
1050

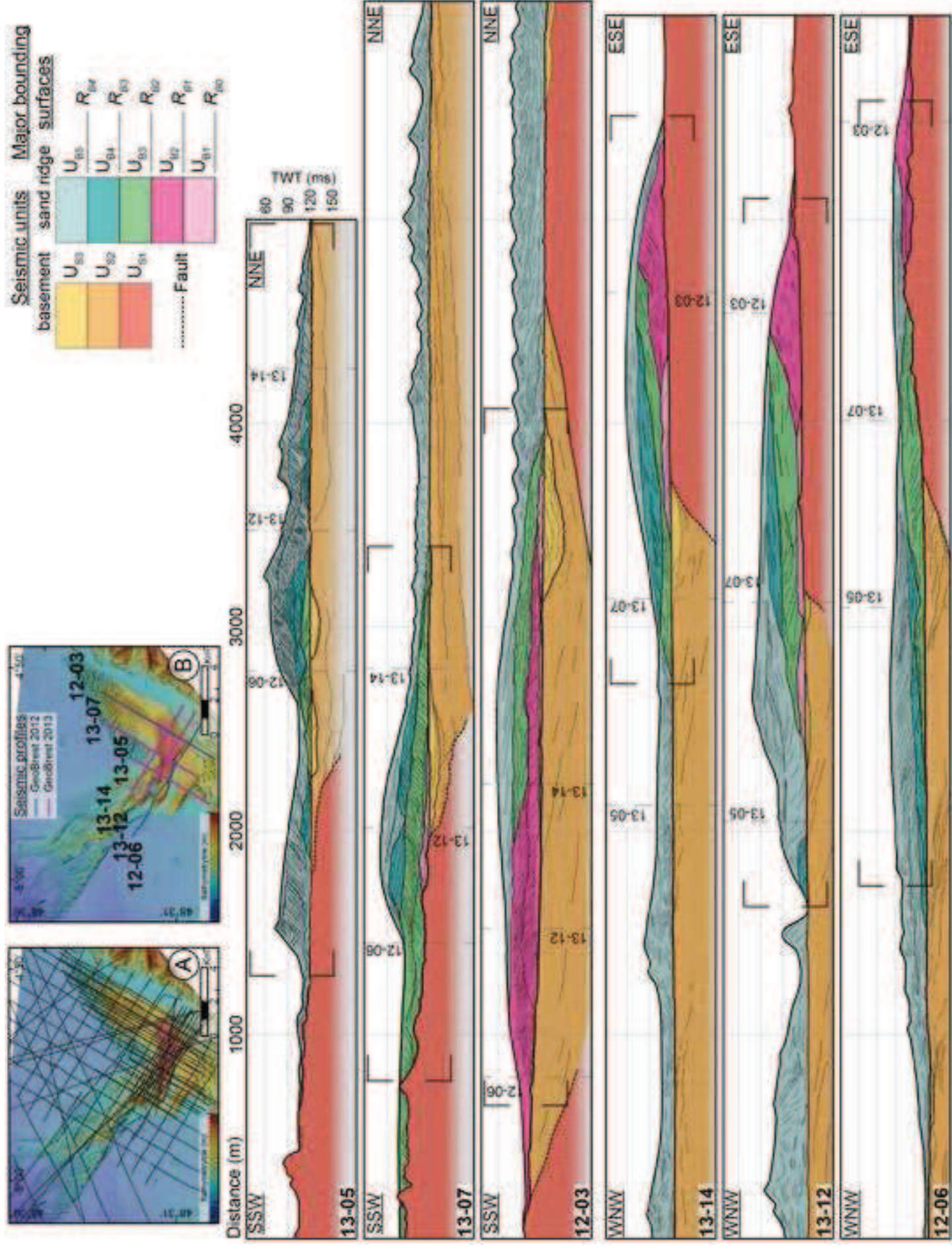
1051 Figure 15. Reconstruction of the last post-glacial sea-level rise through the study area
1052 showing the progressive steps of the ridge growth at -60, -13, -6 and 0 m below the present
1053 sea-level. The emerged lands are in grey scale. The extension of the paleo-ridge is shown in
1054 black and the outline of the present ridge in fine solid black line. The area in grey around the
1055 ridge is expectative and considered as removed by erosion. The tidal connections are
1056 marked by red arrows and the main swell orientations by red dotted lines. The directions of
1057 main sedimentary transport are shown by white arrows.

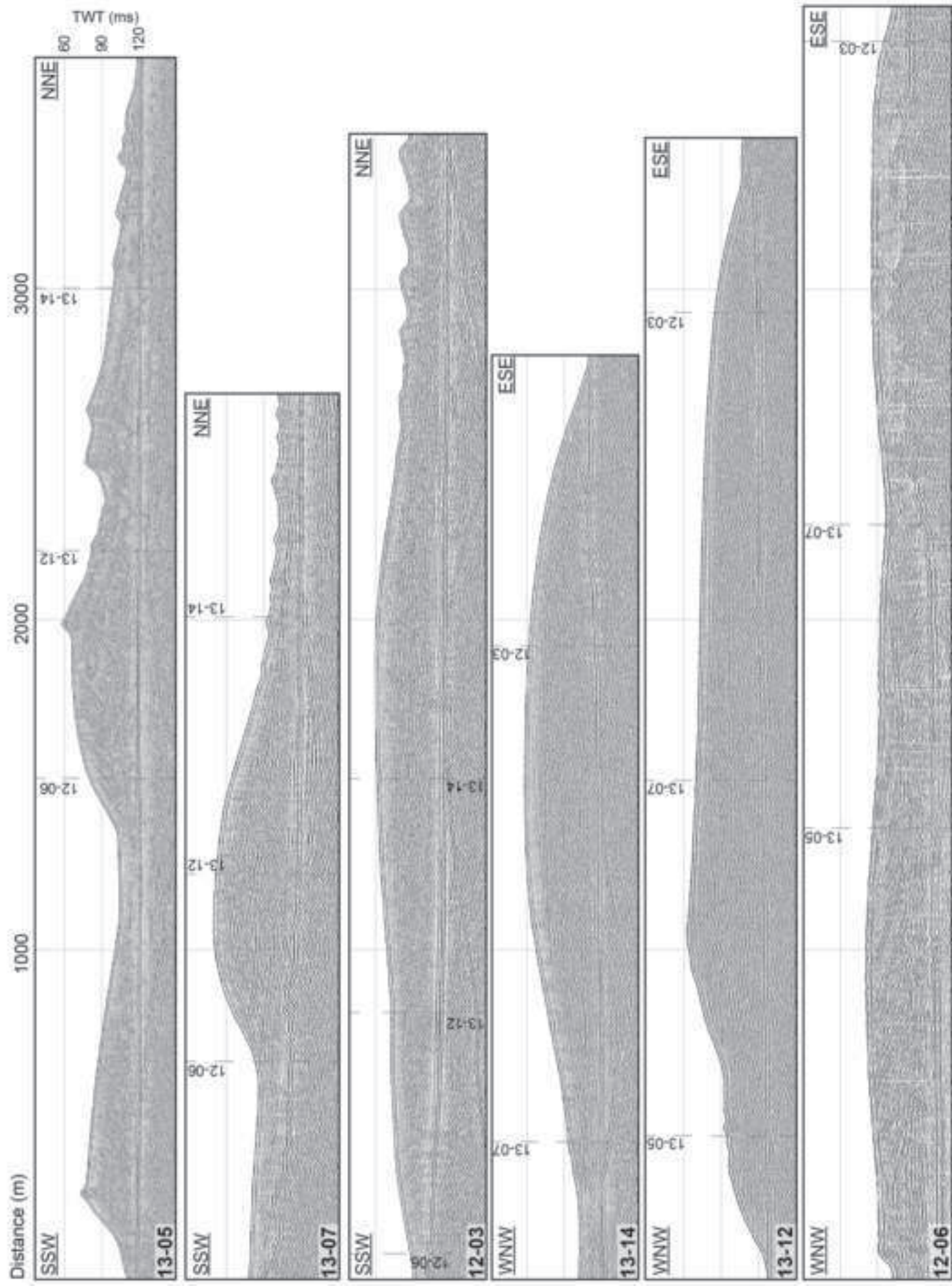
1058

1059









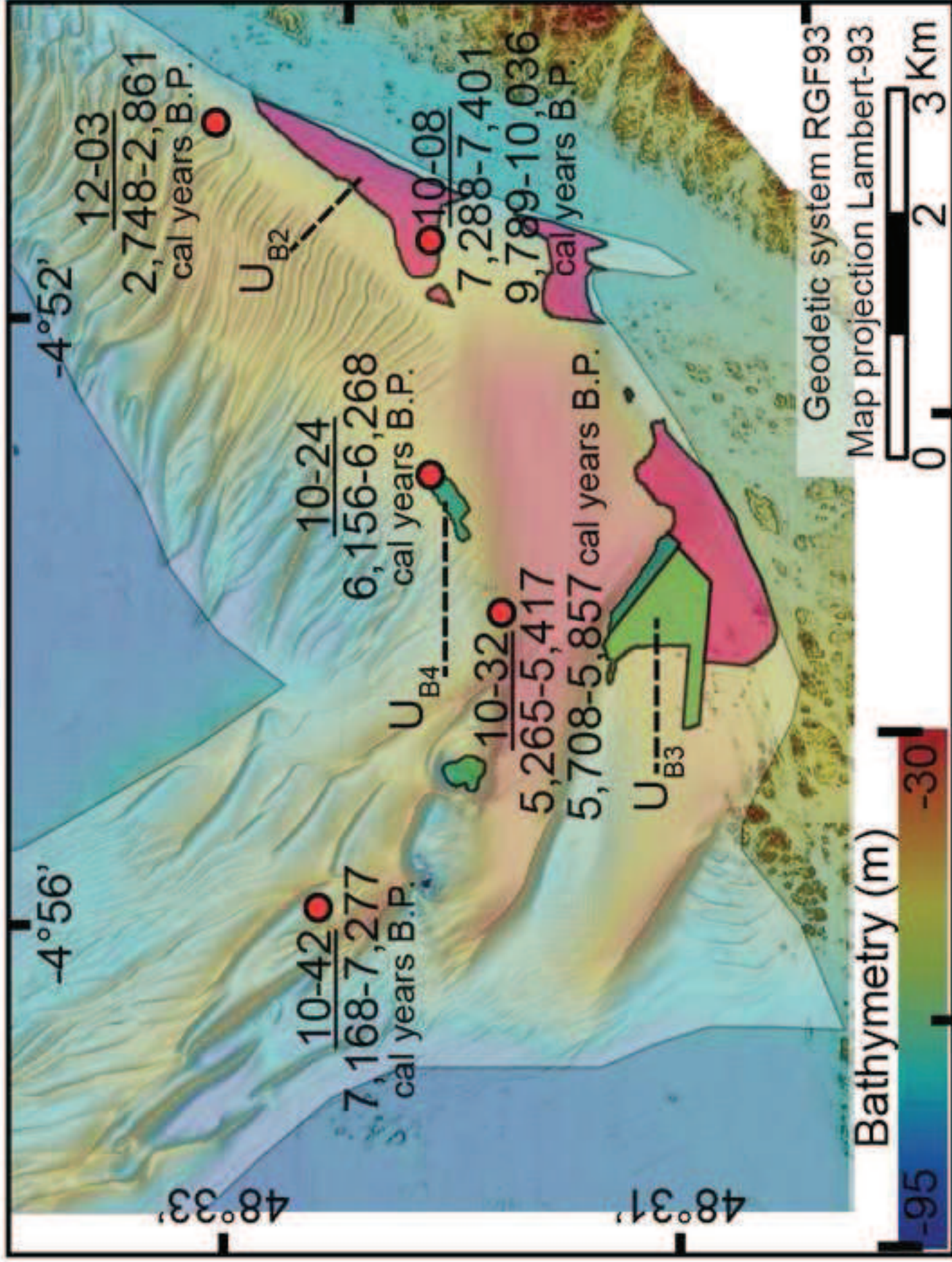
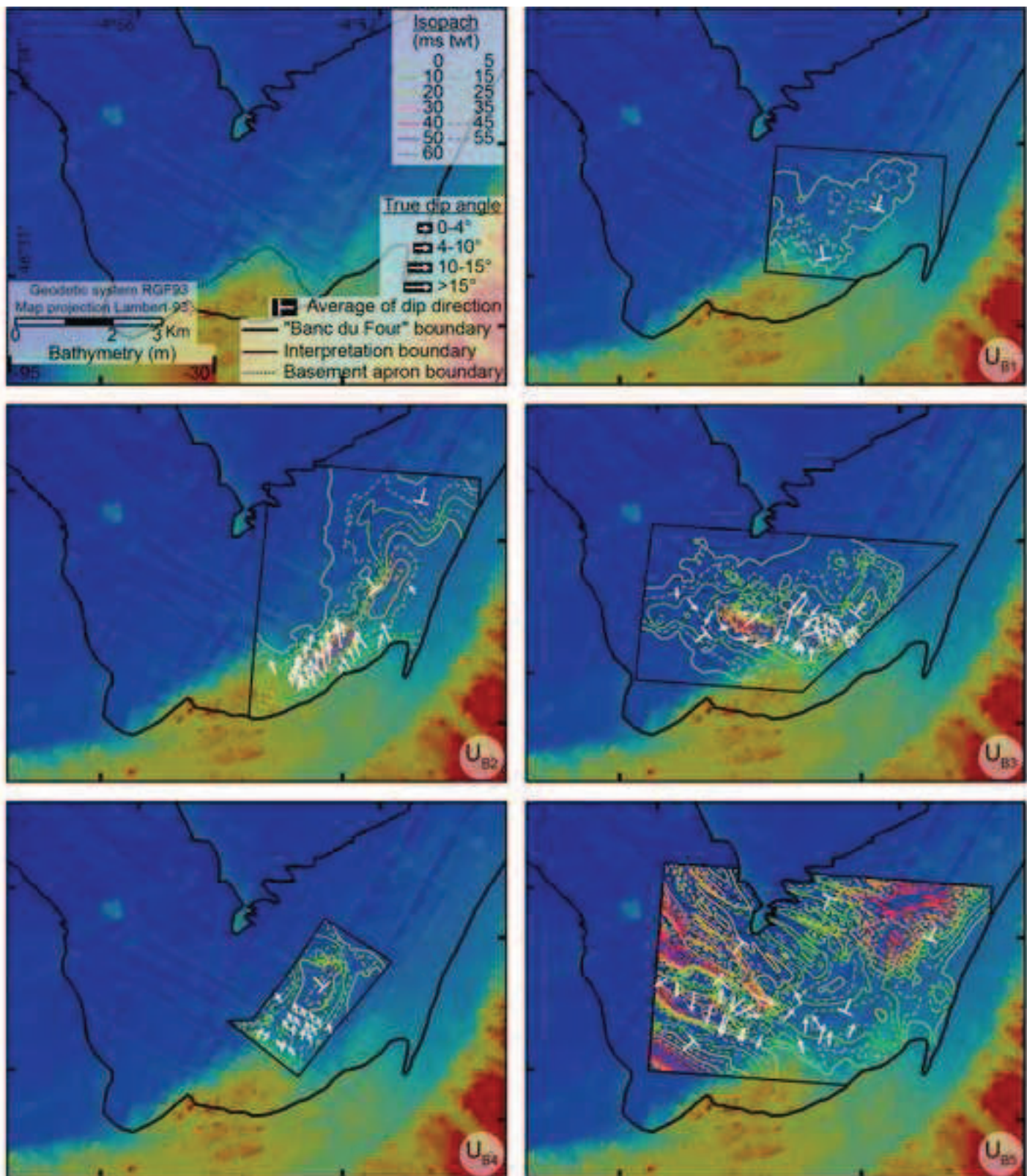
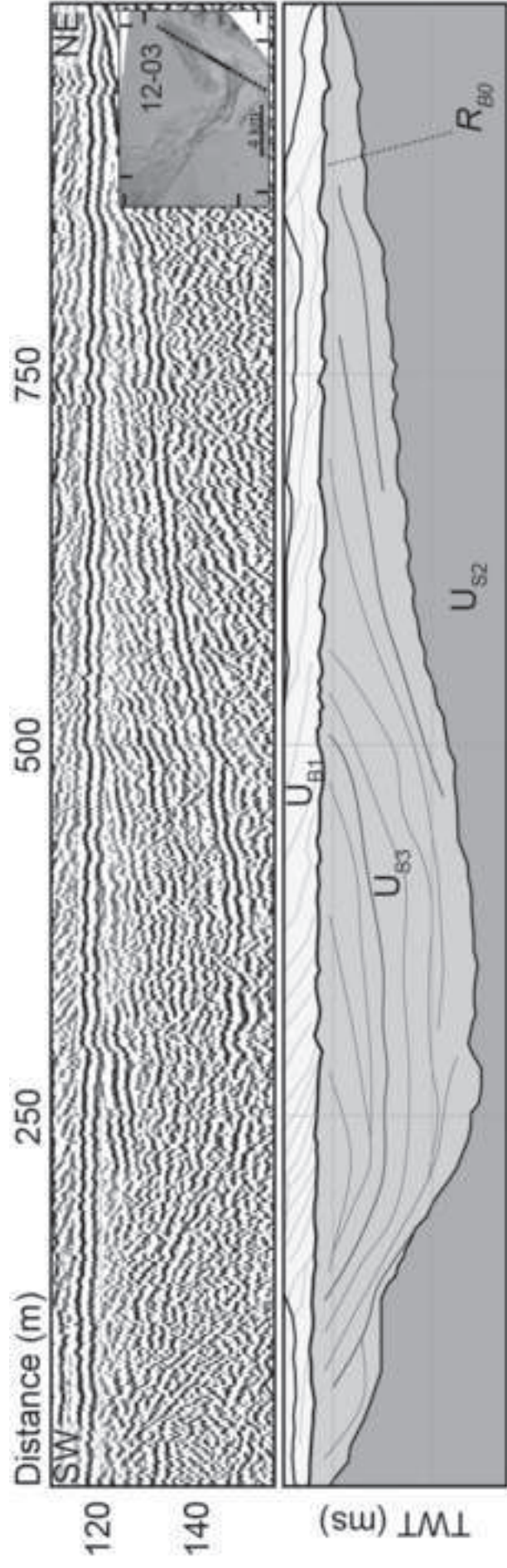
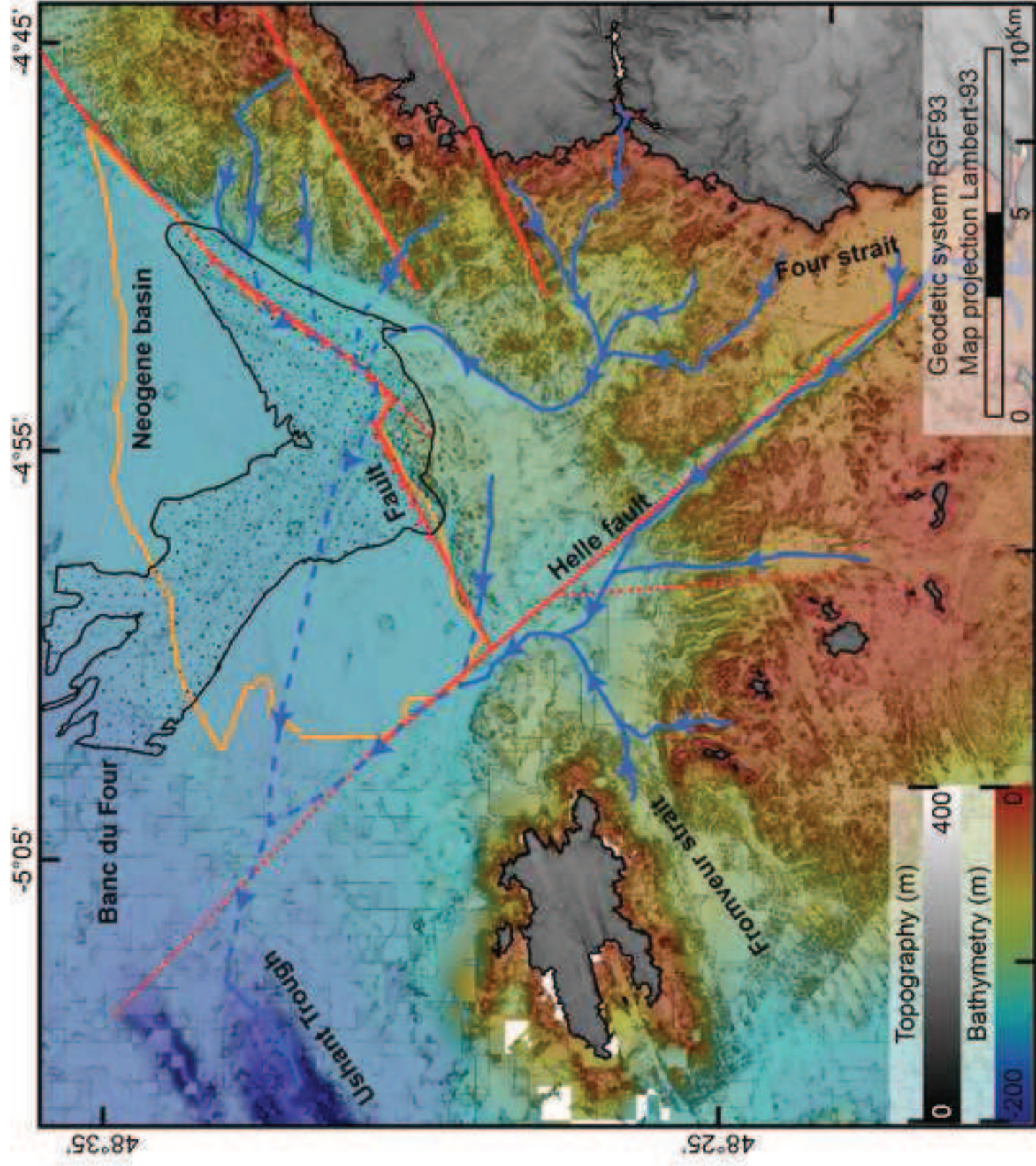
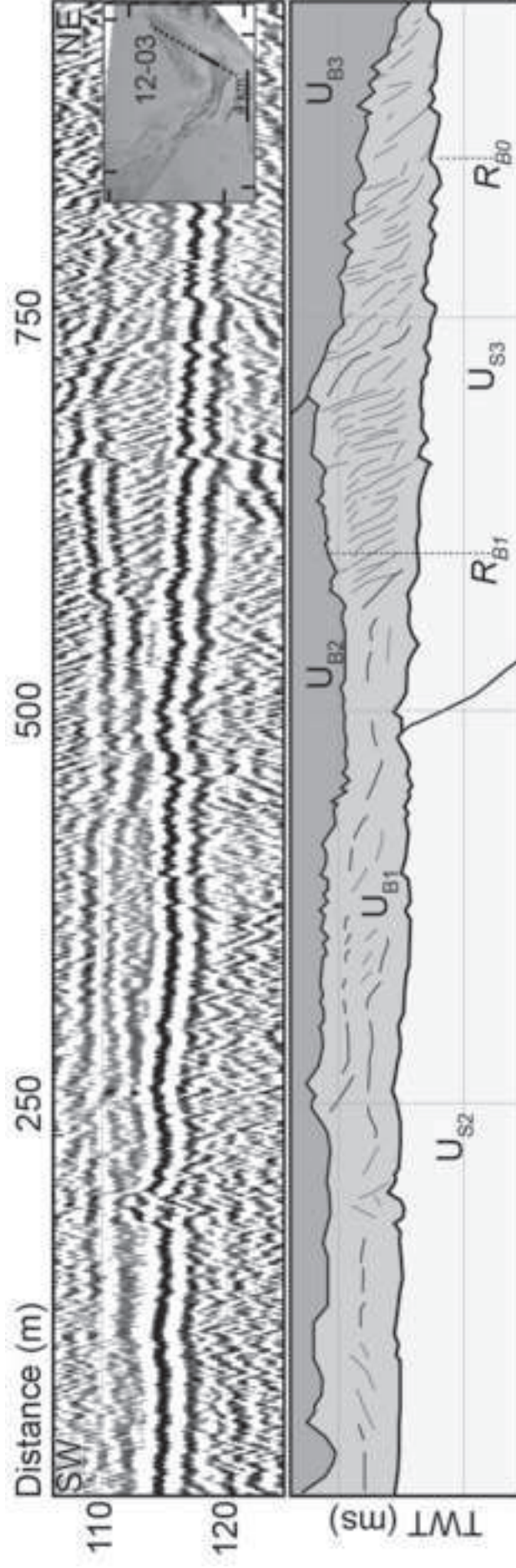


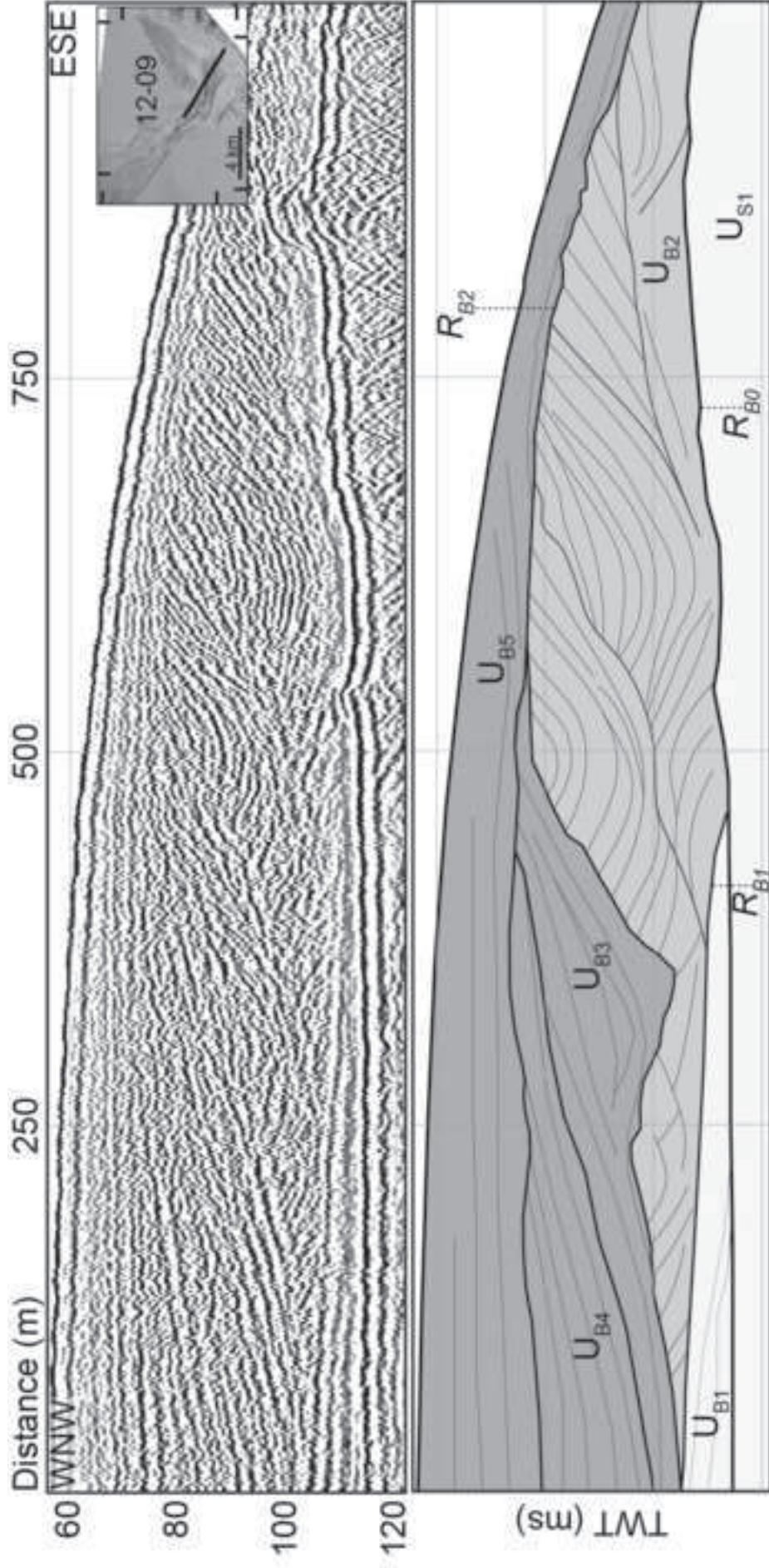
Figure5
[Click here to download high resolution image](#)

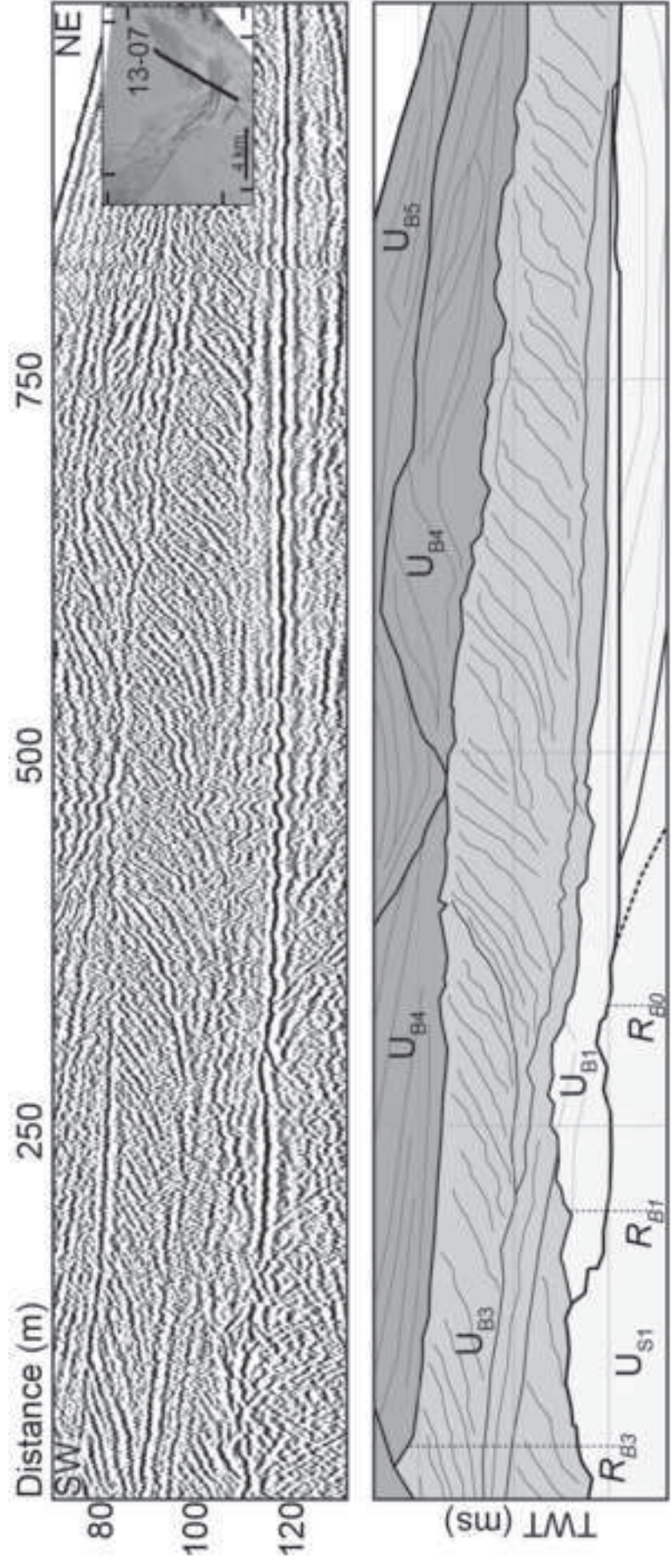


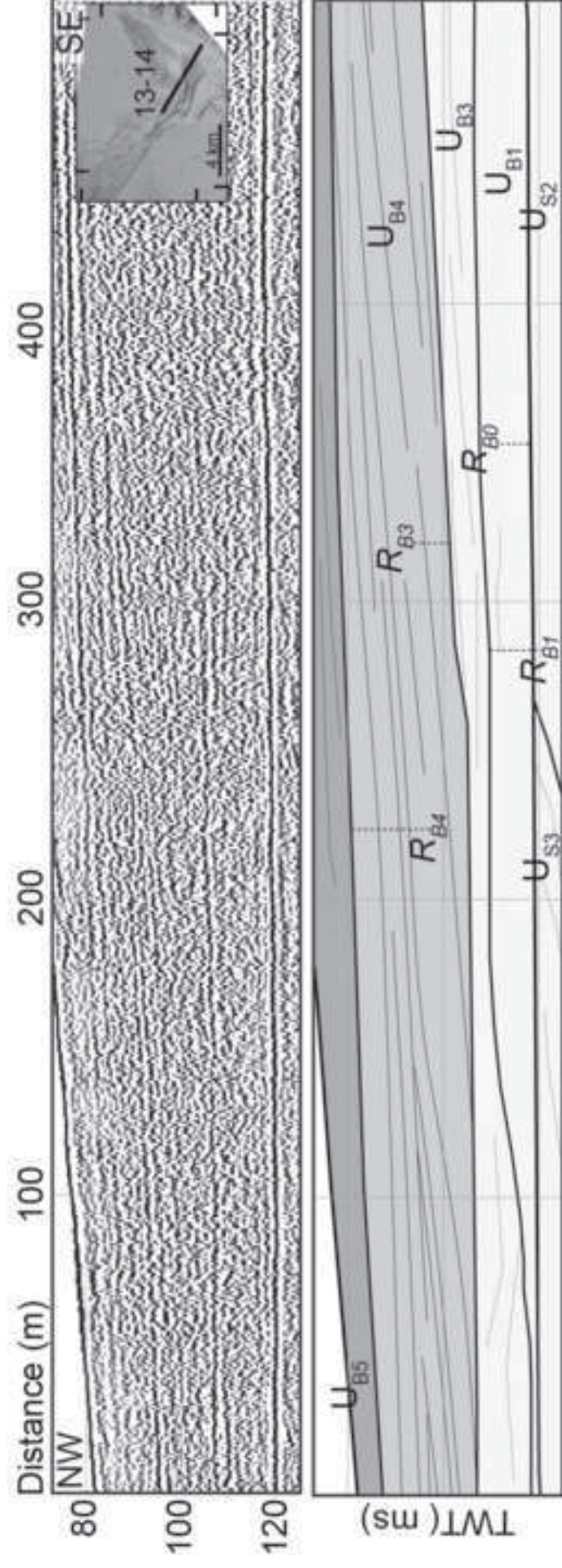


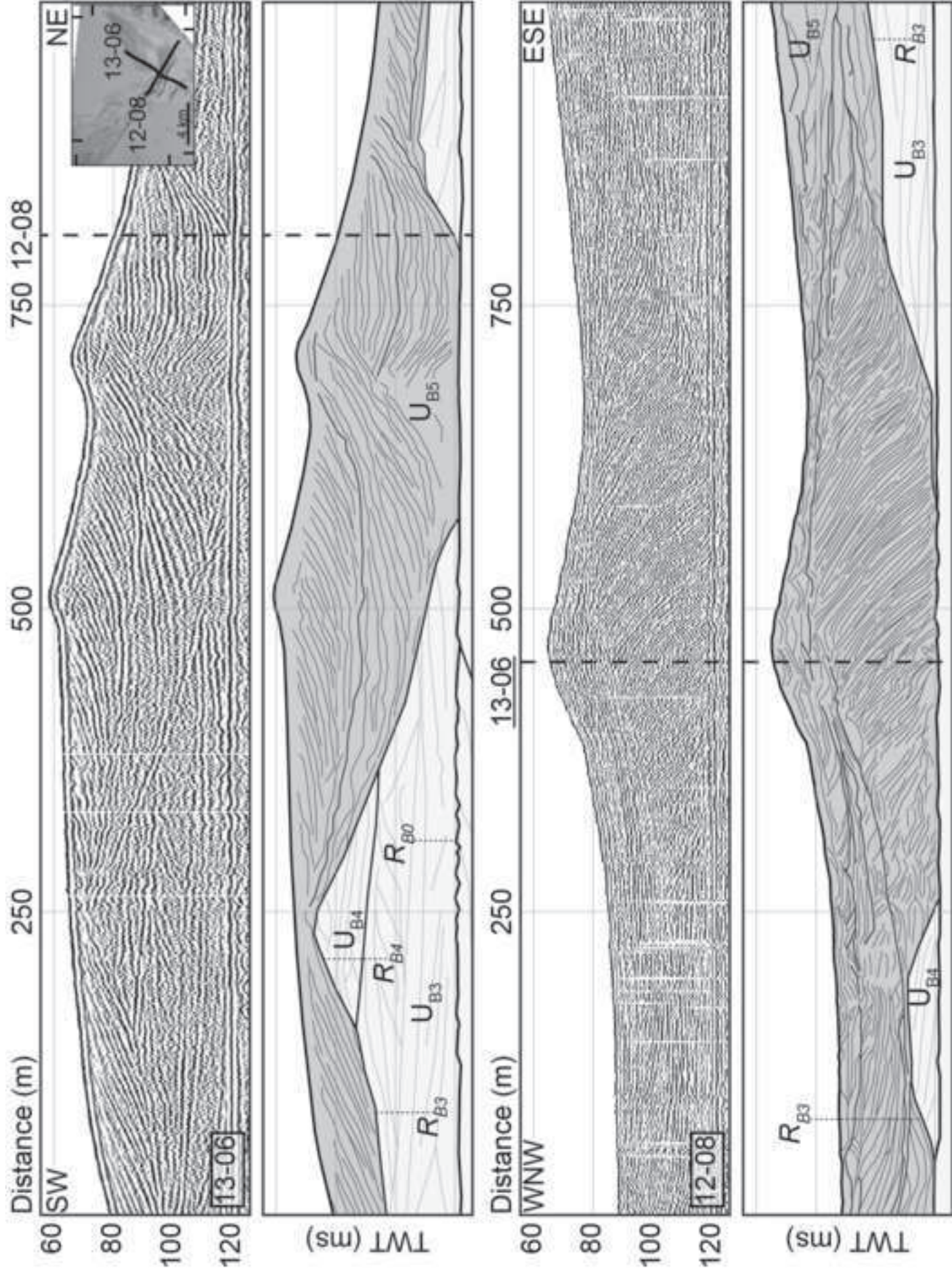


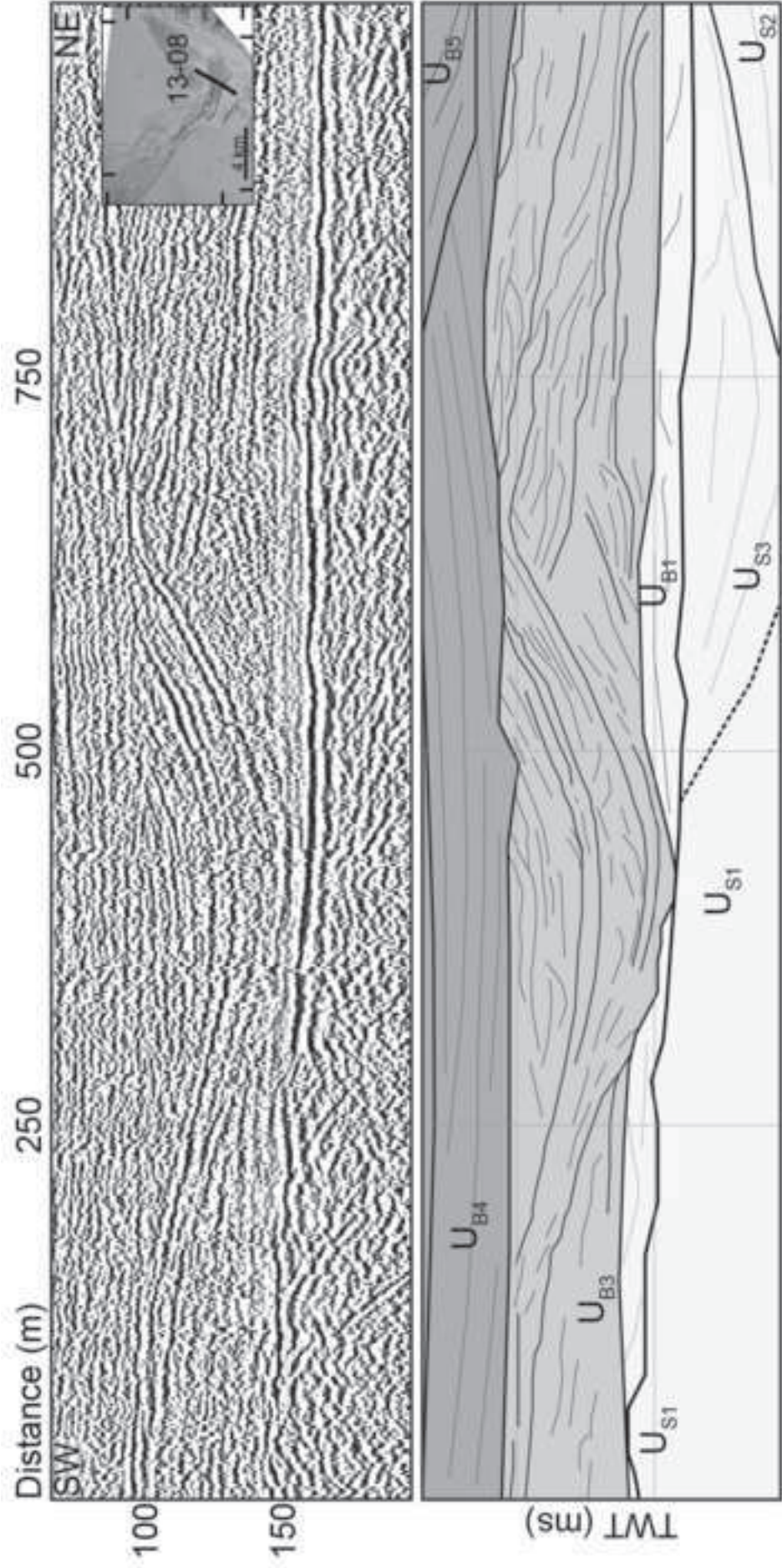


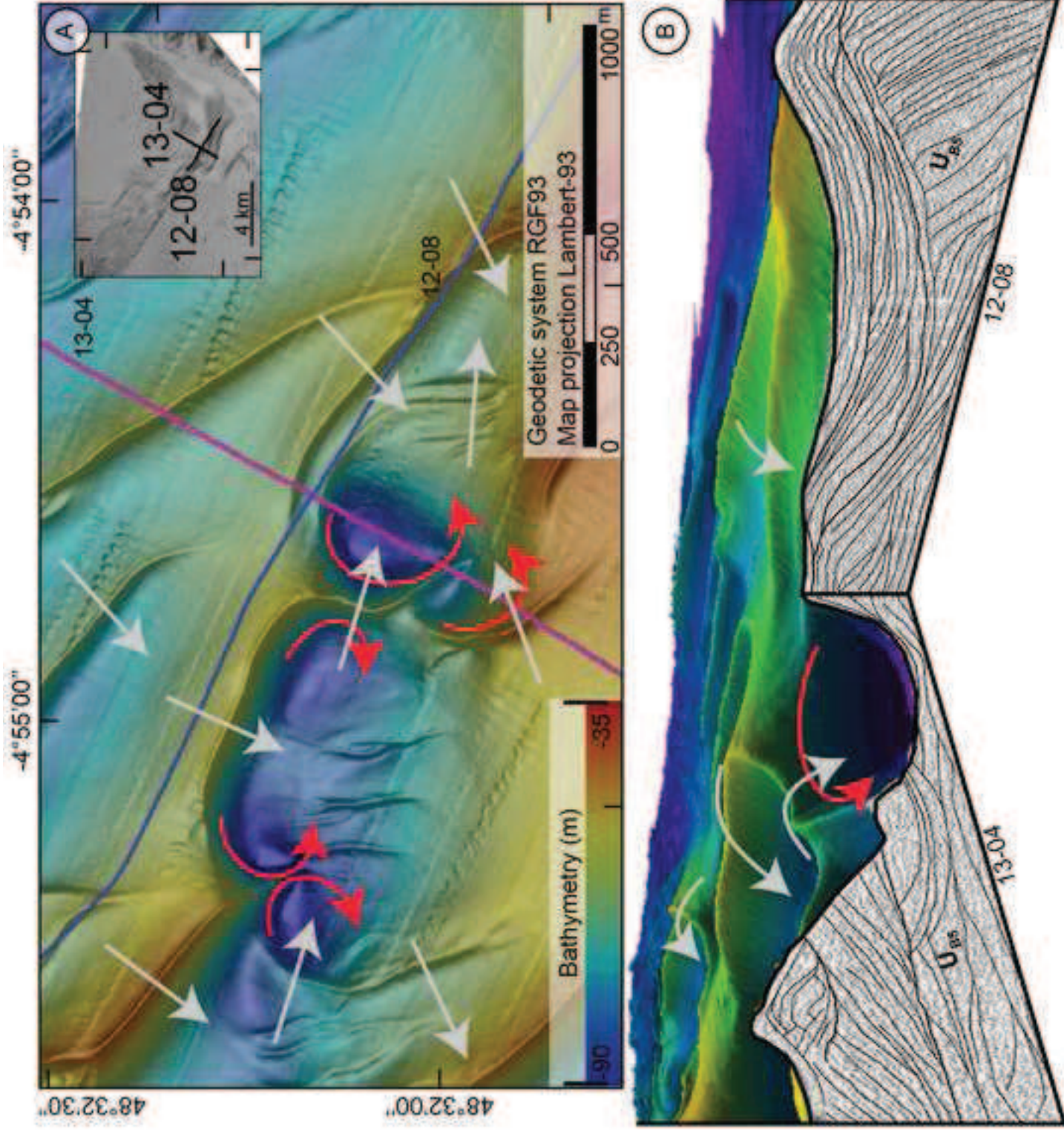


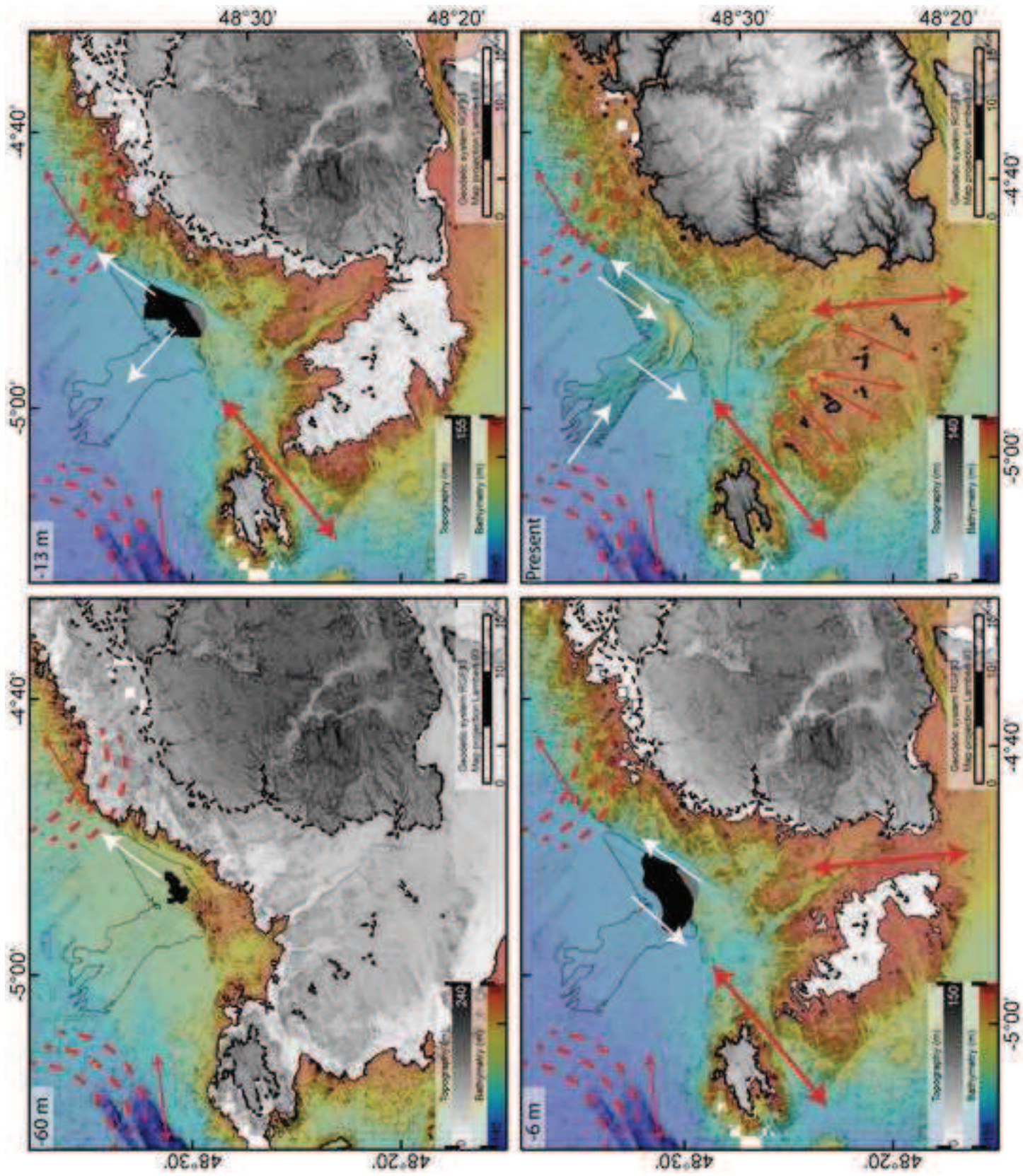












Sample reference	Shell valve preservation (<i>Macoma</i> sp. <i>Glycimeris</i> sp.)	Age AMS C ¹⁴ years B.P.	Calibration 1 σ ($\Delta_R = -40 \pm 42$) cal years B.P.
10-08J	very well preserved	6855 \pm 40	7288 - 7401
10-08V	normal	9175 \pm 35	9789 - 1036
10-24	normal	5815 \pm 30	6156 - 6268
10-32	normal	5010 \pm 40	5265 - 5417
10-32J	very well preserved	5440 \pm 40	5708 - 5857
10-42V	normal	6740 \pm 30	7168 - 7277
12-03	normal	3085 \pm 30	2748 - 2861